EXTRACTION, ISOLATION, CHARACTERIZATION AND APPLICATIONS OF CELLULOSE DERIVED FROM ORANGE PEEL

NG CHOO HUEY

BACHELOR OF SCIENCE (HONS) CHEMISTRY

FACULTY OF SCIENCE

UNIVERSITI TUNKU ABDUL RAHMAN

MAY 2019

EXTRACTION, ISOLATION, CHARACTERIZATION AND APPLICATIONS OF CELLULOSE DERIVED FROM ORANGE PEEL

By

NG CHOO HUEY

A project report submitted to the Department of Chemical Science

Faculty of Science

UniversitiTunku Abdul Rahman

in partial fulfilment of the requirements for the degree of

Bachelor of Science (Hons) Chemistry

May 2019

ABSTRACT

EXTRACTION, ISOLATION, CHARACTERIZATION AND APPLICATIONS OF CELLULOSE DERIVED FROM ORANGE PEEL

NG CHOO HUEY

In this study, cellulose was extracted and isolated from orange peel (OP) via alkaline treatment followed by bleaching process. The orange peel derived cellulose (OPDC) was characterized and compared with microcrystalline cellulose (MCC) by Attenuated Total Reflectance Spectroscopy (ATR), Field Emission Scanning Electron Microscopy (FESEM), particle size analysis, Differential Scanning Calorimetry (DSC) and X-Ray Diffraction (XRD) analysis. ATR spectra for both OPDC and MCC confirm absorption peaks characteristic of cellulose around 3336, 2895, 1639, 1428, 1159, 1027 and 897 cm^{-1}. From the DSC analysis, MCC has higher thermal stability than OPDC. In addition, the results of FESEM showed the microfibrillated cellulose and particle size analysis revealed that OPDC has become micro-sized after pre-treatments. The crystallinity index (CrI) of the OPDC (80.14%) was found to be significantly higher than that of untreated OP

(23.54%). After that, biodegradable blended film with different weight ratio was prepared using OPDC and MCC with polyvinyl alcohol (PVA) by solution casting method. According to the ATR spectra, the shift of the characteristic absorption band and the change in intensity of the band observed in the spectra of PVA/OPDC blended films were similar to that of PVA/MCC blended films. This can confirm the development of new inter- and intramolecular hydrogen bonds and a change in the conformation between PVA and cellulose. Tensile strength and elongation at break of both PVA/OPDC and PVA/MCC blended films were decreased when the cellulose content was increased in the PVA matrix. However, the elastic modulus was increased as the amount of cellulose was increased. By comparison, PVA/OPDC blended film presented higher tensile strength and elastic modulus than PVA/MCC blended film. Based on the natural weathering test, the degradability for blended films were increased with increasing amount of cellulose after exposed to degradation test. The biodegradability of blended film was confirmed by the tiny black spots observed on the surface of the film, which reflect the growth of microorganism. It was further proven by the morphology studies on the surface of the films using FESEM.

ABSTRAK

PENGEKSTRAKAN, ISOLASI, PENCIRIAN DAN APLIKASI SELULOSA YANG DIPEROLEH DARIPADA KULIT OREN

NG CHOO HUEY

Dalam kajian ini, selulosa telah diekstrak dan diasingkan daripada kulit oren (OP) melalui rawatan alkali diikuti dengan proses pemutihan. Kesan selulosa yang diperoleh daripada kulit oren (OPDC) telah dicirikan dan dibandingkan dengan selulosa microcrystalline (MCC) melalui jelmaan spektroskopi Attenuated Total Reflectance (ATR), microskop pengimbasan pelepasan medan (FESEM), analisis saiz partikel, analiss pengimbasan pembezaan kalorimetri (DSC) dan X-Ray analisis (XRD). Spektrum ATR untuk OPDC dan MCC mengesahkan sifat penyerapan selulosa di sekitar 3336, 2895, 1639, 1428, 1159, 1027 dan 897 cm^{-1}. Dari analisis DSC, MCC mempunyai kestabilan terma yang lebih tinggi daripada OPDC. Di samping itu, keputusan FESEM menunjukkan mikroselulosa yang berfibrilasi dan analisis saiz partikel mendedahkan bahawa OPDC telah menjadi bersaiz mikro selepas pra-rawatan. Indeks crystallinity (CrI) OPDC (80.14%) didapati lebih tinggi daripada OP yang tidak dirawat (23.54%). Seterusnya, filem yang mempunyai sifat biodegradasi dengan nisbah berat yang berbeza telah disediakan menggunakan OPDC dan MCC dengan polyvinyl alkohol (PVA) dengan menggunakan kaedah penuangan larutan. Menurut spektrum ATR, cirri pergeseran band penyerapan dan perubahan intensiti band yang diperhatikan dalam spectrum filem PVA/OPDC adalah serupa dengan filem campuran PVA/ MCC. Ini dapat mengesahkan pembangunan ikatan hidrogen inter-dan intramolekul baru dan perubahan dalam konformasi antara PVA dan selulosa. Kekuatan tegangan dan pemanjangan pada takat putus filem adunan kedua-dua filem PVA/OPDC dan PVA/MCC dikurangkan dengan peningkatan kandungan selulosa dalam matriks PVA. Walau bagaimanapun, modulus anjal meningkat dengan peningkatan jumlah selulosa. Sebagai perbandingan, filem campuran PVA/OPDC memberikan kekuatan tegangan dan modulus elastik yang lebih tinggi daripada filem campuran PVA/MCC. Berdasarkan ujian cuaca alam semula jadi, kemerosotan untuk filem campuran telah meningkat dengan jumlah selulosa yang meningkat selepas terdedah kepada ujian degradasi. Biodegradasi filem campuran telah disahkan oleh bintik-bintik hitam kecil yang diperhatikan di permukaan filem, yang mencerminkan pertumbuhan mikroorganisma. Ia dibuktikan lagi oleh kajian morfologi mengenai permukaan filem yang menggunakan FESEM.

ACKNOWLEDGEMENT

First and foremost, I am grateful that I managed to complete my final year project in University Tunku Abdul Rahman Perak Campus. I would like to express my deepest thanks of gratitude to my final year project supervisor, Dr. Ooi Zhong Xian for his valuable guidance and constant supervision as well as his unconditional support in assisting me to complete this project.

It would not be possible to complete my research project without the support and help of the kind people around me in so many ways. I would like to express my special gratitude and thanks to all the staffs in Department of Chemical Science and Faculty of Engineering and Green Technology Utar for giving me such necessary guidance, attention, encouragement and their willingness to share their own experiences and expertise in their respective fields with me.

Last but not least, my thanks and appreciations also go to my beloved family and friends for their endless support, love and all other unnamed who help me directly and indirectly in completing this project.

DECLARATION

I hereby declare that the content presented in this project report has been composed solely by myself, except for quotations and citations which have been duly acknowledged. I also declare that it has not been previously or concurrently submitted, in whole or in part, for any previous application of degree at UTAR or other institutions.

NG CHOO HUEY

APPROVAL SHEET

This project report entitled "**EXTRACTION, ISOLATION, CHARACTERIZATION AND APPLICATIONS OF CELLULOSE DERIVED FROM ORANGE PEEL**" was prepared by NG CHOO HUEY and submitted as partial fulfillment of the requirements for the degree of Bachelor of Science (Hons) Chemistry at Universiti Tunku Abdul Rahman.

Approved by:

____

(Dr. Ooi Zhong Xian) Date :_________________
Supervisor
Department of Chemical Science
Faculty of Science
Universiti Tunku Abdul Rahman

FACULTY OF SCIENCE

UNIVERSITI TUNKU ABDUL RAHMAN

Date: _____________

PERMISSION SHEET

It is hereby certified that **NG CHOO HUEY** (ID No: **15ADB04586**) has completed this final year project entitled "**EXTRACTION, ISOLATION, CHARACTERIZATION AND APPLICATIONS OF CELLULOSE DERIVED FROM ORANGE PEEL**" under the supervision of **DR. OOI ZHONG XIAN** from the Department of Chemical Science, Faculty of Science.

I hereby give permission to the University to upload the softcopy of my final year project in pdf format into the UTAR Institutional Repository, which may be made accessible to the UTAR community and public.

Yours truly,

____

(NG CHOO HUEY)

TABLE OF CONTENTS

CHAPTER

LIST OF TABLES

LIST OF FIGURES

LIST OF ABBREVIATIONS

ATR	Attenuated total reflectance spectroscopy
BFF	Banana frond flour
BOD	Biological oxygen demand
BSG	Brewer's spent grain
CCE	Cold caustic extraction
CCS	Coconut shell powder
CNC	Cellulose nanocrystal
COD	Chemical oxygen demand
CrI	Crystallinity index
CS	Corn starch
DSC	Differential scanning calorimetry
FESEM	Field emission scanning electron microscope
FTIR	Fourier transform infrared spectroscopy
I_{002}	Peak intensity of the 002 lattice plane
I_{am}	Peak intensity of diffraction of the amorphous region
MCC	Microcrystalline cellulose
MSW	Municipal solid wastes
OP	Orange peel
OPA	Oil palm ash
OPDC	Orange peel derived cellulose

RWF	Rambutan skin waste flour
PA	Polyamide
PCL	Polycaprolactone
PE	Polyethylene
PES	Polyester
PET	Poly(ethylene terepthalate)
PLA	Poly(lactic acid)
POPs	Persistant organic pollutants
PP	Polypropylene
PS	Polystyrene
PVA	Poly(vinyl alcohol)
PVC	Poly(vinyl chloride)
SEM	Scanning electron microscopy
UV	Ultraviolet
WVTR	Water vapour transmission rate
XRD	X-ray diffraction

CHAPTER 1

INTRODUCTION

1.1 Background of Study

One of the most consumed and well-known type of fruits around the world is citrus (orange, grapefruit and lemon), due to its useful nutritional properties such as vitamin C, dietary fibres, folic acid and minerals such as calcium and potassium which are of great importance for health. Besides, citrus contains many phytochemicals such as flavonoids, phenolic acids, carotenoids and amino acids, which provides protection against diseases like stroke, gastric, esophageal and colorectal (Roussos, 2011;Zain et al., 2014).

All plant materials including citrus and natural lignocellulosic materials which consist of 3 organic compounds which are cellulose, hemicelluloses and lignin. Lignin is a high molecular weight complex and amorphous polymer with three-dimensional network which is linked by phenylpropane monomers. It provides support to the plant cell wall, microbial resistance and it has hydrophobicity of the cell wall (Jung et al., 2015). Hemicellulose is a complicated carbohydrate polymer and has low molecular weight as compared to cellulose. It consists of Ɗ-Xylose, mannose, L-arabinose, galactose and glucuronic acid subunits which are linked to each other by β-1,4-glycosidic bonds in main chains and β-1,6-glycosidic bonds in side chains (Pérez et al., 2002).

Cellulose is the most abundant renewable resource on Earth, which is found primarily in the cell wall of plants. It is large-molecule polymer composed of repeating units of Ɗ-glucose units joined by β-1,4-glycosidic bonds. The main chemical bond which is present in large amount is hydrogen bond that builds a large network which directly gives the crystalline structure. However, noncrystalline phases are found in cellulose when analyzed by X-ray diffraction, which indicates an amorphous region. This is because the glucose units which have the hydroxyl groups are mostly amorphous (Chen, 2014).

One of the biopolymers on earth is cellulose which is a biodegradable material that may be decomposed by microorganisms in soil to carbon dioxide and water (Zhang et al., 1996). Natural cellulose fibres can be found and isolated from waste plant biomass, which has a wide range of applications which are paper products, films from cellulose acetate, composites, upholstery, cotton and textile materials. Moreover, cellulose derivatives can be obtained from chemical modification of cellulose in which cellulose derivatives are stronger and can be recycled, reproduced as well as biocompatible (Lavanya et al., 2011). For instance, cellulose films, which are produced from cellulose fibres was the first transparent packaging film used for snack foods, biscuits as well as for adhesive tape. Cellophane is a common name for cellulose film which is a renewable resource and biodegradable polymer which has good clarity, glitter and eye-catching colours. Besides, dead fold properties are the main factor which caused the utilization in twist wrapping of sweets and chocolates (Riley, 2012).

Plastics have become one of the most important materials in our lives, such as polyethylene (PE), polyethylene terephthalate (PET), polyvinyl chloride (PVC), polyamide (PA), also known as nylon, polystyrene (PS), polyester (PES), and polypropylene (PP). However, production of plastics from petroleum has raised the environmental pollution due to their non-biodegradable properties, which are highly resistant to natural processes of degradation (Zhang et al., 1996; Prieto, 2016). According to Eich et al. (2015), plastic is considered stable as it requires several hundred years of degradation time depending on the types of plastics. Most of the plastic types are bio-inert and therefore non-biodegradable because of the hydrophobic properties and high molecular weight of synthetic polymers that prevents phagocytosis. As a consequence, the overall decomposition of microbial plastic is low, even though some microorganisms are capable of degrading the plastic.

One of the attempts to overcome the disposal of plastic waste is by producing environmental friendly biodegradable plastic. There are many kinds of biodegradable polymers such as polylactic acid (PLA) and polycaprolactone (PCL) however polyvinyl alcohol (PVA) is the most promising and widely used polymer. PVA is a water soluble synthetic polymer, which is one of the most promising materials among the biodegradable plastic source due to its biodegradability, biocompatibility, high tensile strength, high-modulus and easy to process (Lu et al., 2008; Roohani et al., 2008; Kord et al., 2016). In addition, PVA has thermoplasticity which makes solution casting method to produce film possible (Ooi, 2011). Nevertheless, pure PVA is many times insufficient for its uses due to its brittleness, flammable, poor thermal stability and solvent resistance, which requires the demand of reinforcing agents to improve its properties (Kord et al., 2016).

Eco-sustainable composites can be obtained from the mixture of PVA with natural cellulose fibres. The natural cellulose fibres are compatible with PVA due to the presence of hydroxyl groups which has hydrophilic nature in cellulose, which makes excellent composite properties and good performance (Tan et al., 2015). The uses of PVA include adhesives, paints, textiles, coatings, plastics, membranes, etc (Roohani et al., 2008; Kord et al., 2016). Based on the previous study, PVA was blended with several natural biopolymers to enhance the biodegradability and reduce the cost. For instance, the most widely used and well-known biodegradable polymer in packaging and agriculture industry is PVA/starch blended film (Tang et al., 2008). Moreover, blending of the PVA with lignocellulosic compounds has also been studied such as Suki, Ismail and Hamid (2014) research on PVA/banana frond flour (BFF) biodegradable film, Won et al. (2015) research on biodegradability of the kenaf/soy protein isolate-PVA bicomposites, and Ramaraj (2006) research on PVA/coconut shell powder (CCS) composite films.

1.2 Problem Statement

Citrus fruits belonging to the family of Rutaceae such as lemon, grapefruit, orange, etc account for an important group of fruit crops produced in this world (Mamma, 2008). In the year of 1980 to 2008, there was a sharp increase in the citrus fruit production around the world and continued to increase notably every day which was nearly 120 thousand tonnes in 2014. For instance, orange production in 2014 was about two times more than that in 1980 (Mamma, 2008). Orange is processed to produce juice, yielding huge amount of peel which is a primary waste. This large amount of waste, if disposed improperly on the landfill sites, can pose an environment risk, especially in Malaysia, a country which mainly depends on landfill as a way to throw away solid waste (Wang et al., 2008; Bicu and Mustata, 2011; Malini et al., 2018).

As reported by Renou et al., (2008) and Malini et al., (2018), citrus fruit waste is one of the types of wastes which can easily be found in Malaysia that leads to the generation of leachates. Leachates are the aqueous effluent produced as an effect of biochemical processes and water content in waste’s cells as well as percolation of rainwater through wastes, which can lead to contamination of nearby surface and groundwater if left untreated. Besides, production of leachates can have an effect on the wastewater treatment as leachates have high concentrations of chemical oxygen demand (COD), which is 100-2000 mg/L and biological oxygen demand (BOD), which is 20-1400 mg/L as well as low value of pH which is usually acidic. For this reason, improper disposal of orange peel waste might lead to water pollution.

Moreover, inappropriate landfill disposal causes the release of methane gas, also known as greenhouse gas, and carbon dioxide which then leads to greenhouse effect or global warming. The orange peel waste may also be disposed by incineration which causes air pollution (haze, smog and acid rain) and health risks such as eye irritation, respiratory diseases, cardiovascular damage as well as nervous system damage due to the subsequent generation of pollutants, acid gases, and particulates. Also, without the knowledge of proper waste management from the farmers or workers, disposal of orange peel waste may create the environmental problems (Qdais et al., 2010; Deng et al., 2012).

Over the past 50 years, the production and consumption of plastic has increased due to its desirable properties such as low cost, light weight, good thermal and electrical insulator and ease of manufacture. This increase in consumption has brought about waste management problems with end of life plastics accumulating in landfill as well as natural habitats (O'Brine and Thompson, 2010). After disposal, plastic litter can be introduced into the marine environment, which destroys the ecosystem and harms the marine species. It was reported that substantial amount of plastic waste creates physical hazards for wildlife which could ingest or become entangled in plastic debris. Related environmental impacts also include the accumulation of persistant organic pollutants (POPs) and swallowed plastics mistaken as food (O'Brine and Thompson, 2010; Eich et al., 2015).

According to Adamcová and Vaverkova (2014), the improper disposal of plastics, which are non-biodegradable leads to shortage of the landfill because plastic wastes are estimated to constitute for about 20-30% of the total amount of municipal solid wastes (MSW) landfill site among many wastes. Since plastics cannot be degraded by microorganisms, they tend to remain on the landfill site and take up space, which caused the depletion of landfill. In addition to the landfill problem and also the tendency to harm the marine species, recycling of plastic waste caused to the difficulties of the collection, separation, cleaning as plastic constitutes the diverse types of contamination and complex composite (Ooi et al., 2011b).

1.3 Research Objectives

The main purpose of this research project is to extract, isolate and characterize cellulose from orange peel (OP) and to fabricate the films. The sub-objectives are as follows:

i. To extract and isolate the cellulose from OP by alkaline treatment followed by bleaching process.
ii. To characterize the cellulose derived from OP with regard to its functional group, surface morphology, size of the particle, thermal properties and crystallinity in comparison with MCC.
iii. To prepare different compositions of polymer thin films using OPDC as filler blending with PVA and MCC as filler blending with PVA by using solution casting method.
iv. To characterize the different compositions of PVA/OPDC blended films with regard to its functional group, surface morphology, tensile properties and biodegradability in comparison with PVA/MCC blended films.

1.4 Research Hypothesis

In this research, OPDC obtained after alkaline and bleaching treatment and also MCC will be blended with PVA to cast thin film. Different weight ratio of OPDC and PVA would affect the properties of the blended film in terms of mechanical properties and biodegradability. The hypotheses for this research are:

i. The increasing amount of OPDC and MCC will decrease tensile strength and elongation at break of PVA/OPDC and PVA/MCC blended films.
ii. The increasing amount of OPDC and MCC will increase the elastic modulus of PVA/OPDC and PVA/MCC blended films.
iii. The increasing amount of OPDC and MCC will enhance the biodegradability of PVA/OPDC and PVA/MCC blended films.

1.5 Scope of Study

To achieve the objectives, three scopes have been identified in this research. Firstly, the raw OP and OPDC, which was obtained after alkaline and bleaching treatment, were investigated using Attenuated Total Reflectance Spectrophotometer (ATR), Field Emission Scanning Electron Microscope (FESEM), particle size analyzer, Differential Scanning Calorimetry (DSC) and X-Ray Diffraction (XRD) in comparison with MCC.

Moreover, the effect of different weight ratio of OPDC and PVA on the properties of blended film was studied using Attenuated Total Reflectance Spectrophotometer (ATR), Field Emission Scanning Electron Microscope (FESEM) in comparison to PVA/MCC blended films to gain better understanding of the interaction between polymer and filler.

Next, the mechanical properties of different compositions of polymer thin films such as tensile strength, elongation at break and elastic modulus were investigated and determined. Besides, natural weathering test was carried out to study and compare the biodegradability of polymer films.

CHAPTER 2

LITERATURE REVIEW

2.1 Natural Lignocellulosic Materials

Wood, water plants, agricultural residues, grasses, and other plant substances are sources of lignocellulosics. The most abundant renewable organic matter on Earth is natural lignocellulosic material. Besides the development of high performance materials and composites from lignocellulosic materials in the wood industry, modification can be done to the chemistry of lignocellulosic components to bring about a material that has uniform and consistent properties. For instance, value-added or property-enhanced composites can be produced by changing the properties such as biodegradability, flammability, and degradation as a consequence of ultraviolet light or acids and bases (Rowell, 1992).

Cellulose, hemicelluloses, and lignin are the principal components of natural lignocellulosic materials, which form structures that are rigid and cannot be easily degraded as the structures are connected by different bonding such as covalent and non-covalent bonds. According to literature, the most abundant polymer in lignocelluloses is cellulose, followed by hemicelluloses and lignin (Carr, 2012). However, the compositions of these polymers differ among plant species with age, growth stage, and growing conditions of the plant (Jeffries, 1994; Pérez et al., 2002).

2.1.1 Composition of Lignocelluloses

Cellulose is the major component of plant cell and is the most abundant renewable organic resource on Earth. The linkage found in cellulose is β-1,4-glycosidic bonds, where the oxygen atom connects to C1 of one pyranose ring and C4 of another pyranose ring. There are many intra- and intermolecular hydrogen bonds formed from cellulose chains, which results in the formation of rigid, insoluble microfibrils. Figure 2.1 shows the molecular structure of cellulose (Chen, 2014).

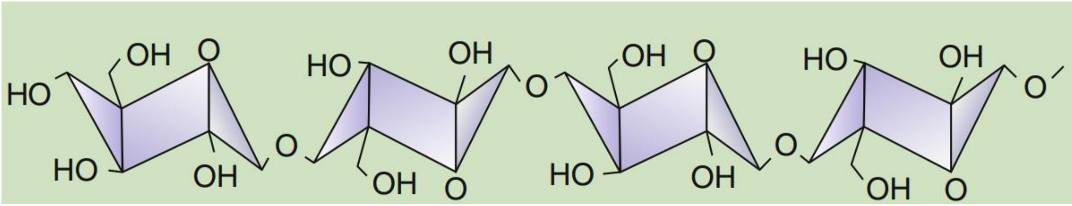

Figure 2.1: Molecular structure of cellulose (Chen, 2014).

Microfibrils are formed by elemental fibrils, which are embedded in a matrix of hemicelluloses and lignin. In addition, microfibrils gather together to form the cellulose fibre. Depending on origin and pre-treatment, cellulose can exist in crystalline form, also known as crystalline cellulose, or in non-organized cellulose chains, called amorphous cellulose. Figure 2.2 shows the structure of microfibril with crystalline and amorphous region (Béguin and Aubert, 1994; Pérez et al., 2002).

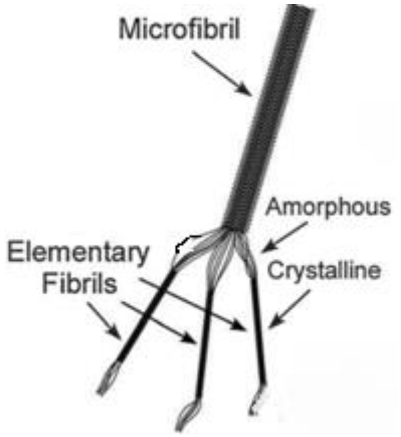

Figure 2.2: Structure of microfibril with crystalline and amorphous region (Moon et al., 2011)

In the secondary walls of plants, hemicellulose is found in association with cellulose in addition to their presence in the primary walls. Hemicellulose, which has a lower molecular weight than cellulose, is composed of complex carbohydrate polymers, with xylans and glucomannans as the main components. In contrast to cellulose, hemicellulose consists of branches with short lateral chains made up of different sugars. Furthermore, they can be easily hydrolyzed as it does not form packed crystalline structure like cellulose, and do not form aggregates, although they are co-crystallized with cellulose. Figure 2.3 shows the structure of hemicellulose (Pérez et al., 2002; Carr, 2012).

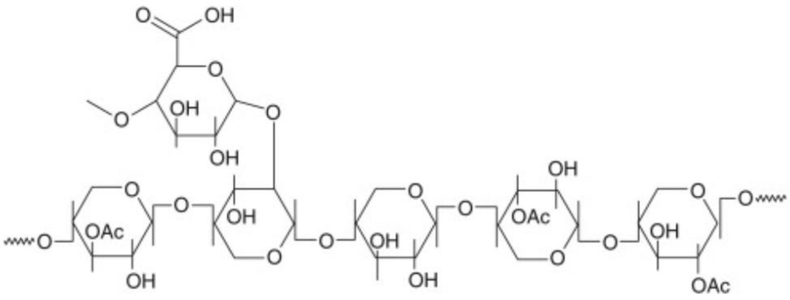

Figure 2.3: Structure of hemicellulose (Gandini and Belgacem, 2013).

In addition to cellulose, lignin, which is found in the cellular cell wall, is the most abundant polymer in nature. Lignin is present as an amorphous matrix, which is made up of phenylpropane units randomly linked together by different types of linkages. The three major monomers are coumaryl alcohol, coniferyl alcohol, and sinapyl alcohol. It provides structural support to the cell wall and also forms a physical barrier which is impermeable. Besides, it is resistant to microbial attack and oxidative stress. Figure 2.4 shows the structure of lignin (Pérez et al., 2002; Carr, 2012).

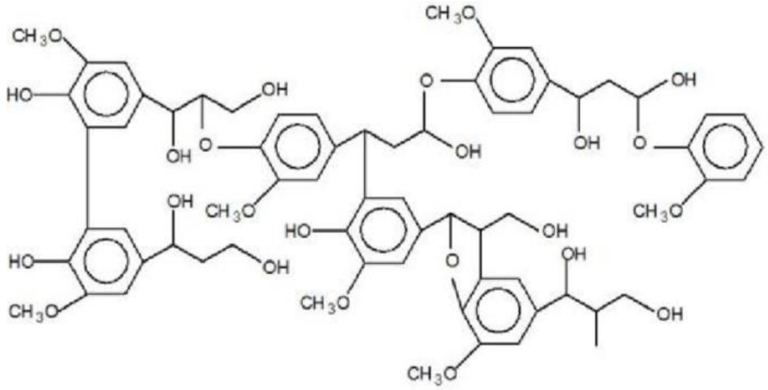

Figure 2.4: Structure of lignin (Price and Kelton, 2013).

2.1.2 Characterization of Lignocelluloses

Fourier Transform Infrared Spectroscopy (FTIR) is one of the common techniques used to characterize lignocelluloses which consist of cellulose, hemicelluloses, and lignin. Figure 2.5 shows the FTIR spectra of pomelo albedo extract. The four samples (a, b, c, and d) do not show a marked difference in the spectra, which suggest that no new substance was formed and no other chemical reaction occurred during the chemical pre-treatment process (Wang et al., 2016; Luo and Wang, 2017). The broad absorption bands around 3300 – 3500 cm^{-1} region indicate the hydrogen bond O – H stretching vibration whereas the absorption peaks around 1610 – 1650 cm^{-1} were the O – H bending of adsorbed water. The absorption peaks near 2900 cm^{-1} correspond to aliphatic C – H stretching vibrations (Lu and Hsieh, 2010; Zain, Yusop and Ahmad, 2014; Luo and Wang, 2017).

One distinguishable vibration peak can be seen in the region around 1734 cm^{-1} on the untreated pomelo albedo, which can be ascribed to the presence of the C=O stretching vibration of the acetyl group of hemicelluloses. The disappearance of this peak on the treated pomelo albedo (Figure 2.5 (b), (c) and (d)) was due to the removal of hemicelluloses after treatment with sodium hydroxide, NaOH (Liu et al., 2004; Sgriccia, Hawley and Misra, 2008; Zain, Yusop and Ahmad, 2014; Luo and Wang, 2017). Next, the absorption peaks around 1230 – 1240 cm^{-1}, which indicate the C – O stretching of the aryl group of lignin has become smaller on the treated FTIR spectra. This portrays the partial removal of lignin from the pomelo albedo surface (Liu et al., 2004; Sgriccia, Hawley and Misra, 2008).

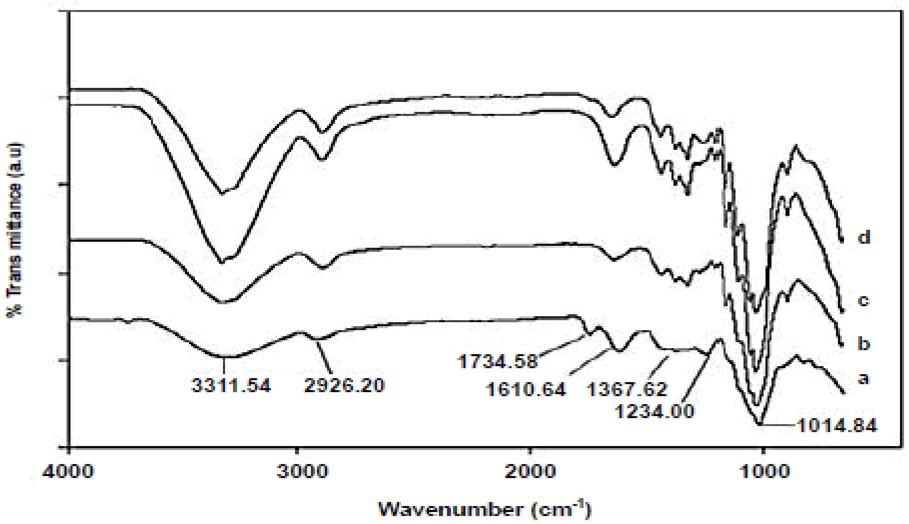

Figure 2.5: FTIR spectra of (a) untreated pomelo albedo, (b) alkali treated pomelo albedo, (c) bleached pomelo albedo (cellulose) and (d) acid hydrolysed pomelo albedo (nanocellulose) (Zain, Yusop and Ahmad, 2014).

2.2 Citrus Waste (Orange Waste)

While citrus waste is greatly produced, the disposal methods used still remain unsatisfied. Improper disposal of citrus waste can be harmful for ruminants, can lead to soil salinity, and are not economically feasible (Bátori et al., 2017). Citrus waste is a globally diverse and environmentally challenging waste which is underutilized (Balu et al., 2012; Bátori et al., 2017). Over the world, sweet oranges are the most commonly grown tropical fruits among citrus fruits. For instance, industrial orange processing, which produces orange juice generates about 50-60% of citrus peel waste, which consists of peel, seeds and membrane residues. Orange waste not only consists of cellulose, hemicellulose, and lignin but also contains pectin, soluble sugars, protein, ash, fat, and flavanoids, which have been shown to be significance to variety yet imperfect disposal and recovery applications (López, Li and Thompson, 2010).

As reported by Bátori et al. (2017), citrus waste consists of many valuable polymers, which can be utilized as a biobased and biodegradable film for food packaging. For instance, orange waste has already been applied as reinforcement in petrochemical or biobased matrices, where pectin-based composites with different reinforcing substances have been produced and cellulosic plant fibres have attracted much attention because of their excellent mechanical properties as a potential substitute for glass fibres in biocomposites. The study on the orange waste film represents competitive mechanical properties with other types of plastic products.

2.3 Cellulose Extraction

Cellulose, which can be extracted using different methods from a wide range of plants and animals has attracted growing interest because of their distinctive characteristics such as high specific strength, good thermal properties and low cost. For instance, extraction of cellulose particles from cellulose microfibrils may involve any pre-treatment (alkaline treatment), dissolution or deconstruction processes (Moon et al., 2011; Lani et al., 2014). In general, cellulose extraction from different plants includes the removal of hemicellulose, lignin, and pectins (Mzimela, 2018).

2.3.1 Dewaxing Solvent

In organic solvents such as ethanol and toluene, organic molecules found in fruit peels like orange peels or banana peels can be extracted. Besides, the treatment with organic solvents not only removes the wax of fruit peel but also loosen the bonds between chain molecules. As mentioned in the literature, ethanol removes hydrophilic compounds such as pigments cellular debris while toluene preferably extracts the hydrophobic molecules such as wax and oils. It was also reported that organic solvent extraction reduces the colouring of the peel and also softens it (Naz et al., 2016).

For instance, dewaxing of bamboo fibre was performed by Soxhlet extraction method using 400 mL of toluene and 200 mL ethanol with the ratio 2:1 at 250˚C for 2 hours. The extraction process was continued until the colour mixture disappears (Liew et al., 2015). According to another literature, 30 g of grounded peel was soaked in ethanol and toluene solution with the ratio 2:1 for 1 day. The mixture was then filtered and the residue was dried at room temperature (Hariani, Riyanti and Asmara, 2016; Naz et al., 2016).

2.3.2 Alkaline Treatment

In an alkaline medium such as sodium hydroxide (NaOH) or potassium hydroxide (KOH) solution, hemicellulose is readily hydrolyzed and has greater solubility than cellulose. Hence, alkaline treatment is one of the common methods to extract hemicelluloses (Egüés et al., 2012; Chen, 2014). For instance, treatment of pomelo albedo with 4 wt% NaOH under reflux condition was carried out for 2 hours to remove the hemicellulose which dissolved in the solution. The mixture was then rinsed with distilled water until a neutral pH was obtained (Zain, Yusop and Ahmad, 2014).

In addition, the surface tension between the natural fibres and polymer matrices can be lowered by modifying the surface of the fibre using alkali solution. The interface adhesion between the natural fibres and polymer matrices can also be increased. After treatment with 5 wt% and 10 wt% alkali solution, the materials in the interfibrillar region, which joined the fibres in grass, were etched away. As the concentration of alkali solution and treatment time was increased, more hemicelluloses and lignin was etched. As reported by the researchers, the surface of the fibre was clean and only a small amount of materials was left in the interfibrillar region. Moreover, the interaction between fibres became lesser after the removal of hemicelluloses, which led to the easy separation of the fibres (Liu et al., 2004).

Alkali treatment using NaOH and KOH can also destroy hydrogen bonds and hydrolyze ester bonds which cause the cellulose to swell and cellulose crystallinity to decrease. Hence, this is a favourable method for the extraction and solubilisation of non-cellulosic binding materials like hemicellulose (Abdel-Halim, 2014; Wei et al., 2018). According to Hariani, Riyanti and Asmara (2016), the hemicellulose in kepok banana peel was removed by using 4 wt% of NaOH and stirring for 4 hours at 60˚C. The mixture was then filtered and washed with distilled water until it reaches pH 7.

Furthermore, alkaline treatment can affect the surface morphology of fibres. According to Figure 2.6, the untreated fibre surface was smooth. Meanwhile the wrinkle on the surface (b-f) became more prominent and the microfibril aggregates can be obviously observed in addition to the presence of pores between the aggregates. Hence, the rougher surface of fibre was a consequence of removal of impurities, non-cellulosic materials and inorganic substances found on the fibre surface at higher NaOH concentration (Saha et al., 2010; Liu et al., 2013; Chen et al., 2017).

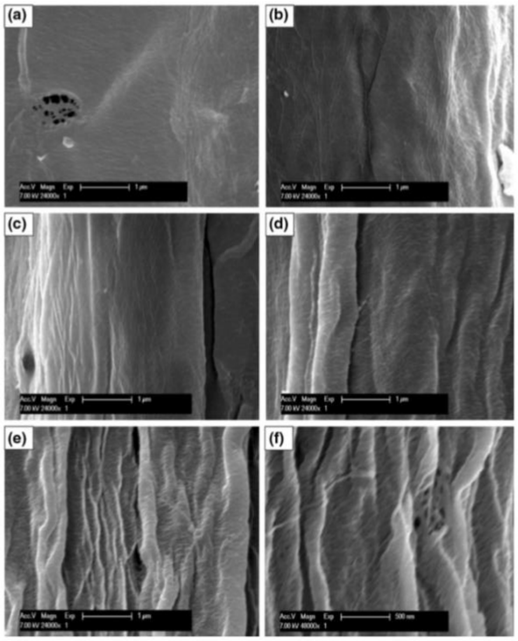

Figure 2.6: SEM images of the surface morphology of each bamboo fibre treated with different concentrations of NaOH solutions, where (a) untreated, (b) 6 wt%, (c) 8 wt%, (d) 10 wt%, (e) 15 wt%, and (f) 25 wt% at high magnification (Chen et al., 2017).

Another method to remove hemicellulose is the combined concept of cold caustic extraction (CCE) and mechanical refining. The removal of hemicellulose during the CCE process involved the swelling of fibres in alkali solution, diffusion of hemicelluloses, where it passed through the pores in the wall of the fibre, and lastly the dissolution process in the bulk phase (Li et al., 2015). To increase the rate of diffusion of hemicellulose, mechanical refining was carried out to enlarge the size, volume and specific surface area of the fibre pores. According to literature, mechanical refining can enhance the porosity of the fibre wall as the internal bonds were broken and the fibre wall was delaminated (Grönqvist et al., 2014; Li et al., 2015).

2.3.3 Bleaching Treatment

After the removal of hemicellulose through alkaline treatment, the subsequent bleaching treatment facilitates the removal of lignin in the fibre. Most studies used sodium chlorite ($NaClO_2$) solution as the bleaching agent (Mzimela, 2018) because high whiteness of cellulose can be obtained without degradation. Moreover, bleaching treatment with $NaClO_2$ is simple because it requires only mild rinsing as fibre-susbstantive alkali is not used (Choudhury, 2011).

Sodium chlorite is a moderate-strength acid, which is only active in acidic medium. When sodium chlorite is activated, decomposition of chlorous acid into chlorine dioxide, chlorate, chloride and oxygen will occur, which is shown by the chemical Equations 2.1-2.3. However, the reaction is pH dependent. Since the solution decomposes slowly at above pH 5.0 and becomes stable in alkaline medium, the bleaching treatment with sodium chlorite must be acidified using organic acids like acetic acid as activator (Choudhury, 2011; Abdel-Halim, 2013).

$$4ClO_2^- + 2H^+ \rightarrow 3ClO_2 + Cl^- + 2OH^- \qquad \text{(Equation 2.1)}$$

$$3ClO_2^- \rightarrow 2ClO_3^- + Cl^- \qquad \text{(Equation 2.2)}$$

$$ClO_2^- \rightarrow Cl^- + 2O \qquad \text{(Equation 2.3)}$$

For instance, empty fruit bunch fibres were boiled in 0.7% (w/v) of $NaClO_2$ solution in an acetic buffer and stirring for 2 hours at about 80˚C. This process was repeated for several times until the fibres turned white. The bleached cellulose was then washed using distilled water for a few times (Lani et al., 2014; Berglund et al., 2016).

Hydrogen peroxide (H_2O_2) bleaching is another oxidative bleaching agent in addition to sodium chlorite. In contrast to sodium chlorite, hydrogen peroxide solution is unstable in alkaline medium, requires a stabilising agent and comparatively expensive (Choudhury, 2011). Hydrogen peroxide is well-known as an environmental friendly bleaching agent because only oxygen and water are produced during the decomposition reaction, which is safe to carry out in an open vessel (Mussatto, Rocha and Roberto, 2008; Choudhury, 2011).

The equilibrium of H_2O_2 shifts to the formation of main active species in peroxide bleaching, which is the hydroperoxide anion (-OOH). According to literature, the reaction of lignin with hydroperoxide anion is irreversible, which results in the permanent removal of majority of the chromophoric groups found in the lignin. (Brooks and Moore, 2000; Mussatto, Rocha and Roberto, 2008).

According to Mussatto, Rocha and Roberto (2008), the bleaching process of brewer's spent grain (BSG) was performed in three stages, where the first two stages was done by using hydrogen peroxide, and the last stage involved only a sodium hydroxide solution. Firstly, 0.07 N NaOH solution was used to adjust the pulp slurry to 10% consistency, which was then mixed with 5% H_2O_2 with stirring for 40 minutes at 70˚C. The pulp was filtered, washed using distilled water, and dried overnight at room temperature. This step was carried out for two consecutive times. Next, 0.25 N NaOH solution was mixed with the pulp and stirring for 1 hour at 70˚C. To remove the residual alkali, the bleached pulp was washed with distilled water for several times. As reported by other researchers, high temperature leads to the instability of hydrogen peroxide. For instance, the duration of bleaching treatment will be very long except for temperature of above 80˚C for natural and man-made fibres (Choudhury, 2011).

2.4 Research on Natural Fibre Reinforced Poly(vinyl alcohol)Based Composites

Few years back, increased in the pollution or environmental issues due to heavy use of plastics have gained the attention of researchers to produce environmental friendly composites. One of the explorations was the usefulness of natural fibres as reinforcement in polymers and composites (Rahman, Afrin and Haque, 2014; Ching et al., 2015; Sreekumar et al., 2018).

Natural fibres from cereal straw, leaf, wood, seed or fruit are commonly used in composites due to their relative cheapness, availability, biodegradability, renewability with production requiring a small amount of energy, and sustainability. In addition to natural fibres, agro-wastes like rice husks, oil palm and sugarcane cultivation, as well as wastes produced from rubber plants (e.g empty fruit bunches) have been considered. Besides, biopolymers such as cellulose and starch, which are obtained from biomass extraction, are being used in the development of biocomposites (John and Thomas, 2008; Tan et al., 2015; Naduparambath et al., 2018).

According to John and Thomas (2008), natural fibres can be considered as naturally occurring composites, which consist largely of cellulose fibrils embedded in lignin matrix. The cellulose fibrils are aligned along the length of the fibres that provide rigidity, high tensile and flexural strengths. The efficiency of natural fibre reinforcement is associated to the nature of cellulose as well as its crystallinity. Cellulose, specifically α-cellulose, hemicellulose, lignin, pectins, and waxes are the major constituents of natural fibres.

For production of eco-friendly and green composites, it is preferable to add the natural fibres in biodegradable polymers such as poly(vinyl alcohol) (PVA), starch, and poly(lactic acid) (PLA) (Sreekumar et al., 2018). Among these polymers, PVA is preferable to substitute the use of non-degradable plastics and synthetic polymers like polyolefin and polystyrene (Ooi et al., 2012a). PVA is biodegradable since it is readily consumed by microorganisms and enzymes when exposed to the environment. However, researchers reported that PVA has low biodegradability due to the joining of backbones of vinyl polymer by the carbon-carbon bonds (Ishigaki et al., 1999; Ooi et al., 2012b).

Next, PVA is a well-known polymer for its excellent properties such as water soluble, ease-to-use and resistant to chemical (Rahman, Afrin and Haque, 2014). PVA has a wide range of applications in the agricultural and packaging industry due to its good thermal stability, flexibility, transparency, toughness, and biocompatibility (John and Thomas, 2008; Naduparambath et al., 2018; Tan et al., 2015). Since PVA is costly, it is suitable to be blended with low cost natural polymers or natural fibres like cellulose to form biodegradable plastic film (Ooi et al., 2012b; Tan et al., 2015; Sreekumar et al., 2018).

2.5 Plasticizer

Plasticizer like glycerol is an additive which was used to provide flexibility and help to soften the PVA blended films. However, the tensile strength of the films was reduced though the plasticizing effect greatly improved the elongation at break.

Examples of other types of plasticizers are urea and sorbitol (Ooi et al, 2012a and 2012b). Glycerol is a typical glass-forming material. It has the strong ability to connect with polysaccharide matrix via hydrogen bonding interaction due to its multi-hydroxyl moiety structure. Hence, applications of glycerol in blending systems such as PVA/starch, PVA/rambutan skin waste flour (RWF), PVA/chitosan, and PVA/oil palm ash (OPA), which were prepared by solution casting method, have significantly enhanced their chain mobility, mechanical flexibility and ductility (Liang et al., 2009; Zhou et al., 2009).

According to literature, glycerol-plasticized PVA blended films has higher elongation at break and lower tensile modulus in contrast to sorbitol-plasticized PVA blended films. The lower tensile modulus was due to the hygroscopic character of glycerol that tends to give extra water into the film matrix. Moreover, the water vapour transmission rate (WVTR) of glycerol-plasticized PVA blended films was higher because glycerol greatly enhanced the molecular mobility and free volume between polymer chains. This was attributed to the lower molecular weight of glycerol (92 dalton). Since glycerol has greater molar content per unit mass, it provides more active sites by exposing its hydroxyl groups to interact with water by hydrogen bonds in which the water molecules could be adsorbed (Mali et al., 2005; Ooi et al., 2012b). WVTR is the capability of water vapour to penetrate through the PVA blended films (Ooi et al., 2012b).

2.6 Solution Casting Method

One of the common methods to produce biodegradable plastic film is the solution casting method. Laboratory scale composite thin films can be easily prepared by using this method. This method not only provides the film with uniform thickness, optical purity, low haze, and isotropy, but it is also a low temperature process. However, it is a slow process and is usually limited to laboratory scale process (Oksman et al., 2014).

To obtain films which are well-adhered to substrate, defection-free, and uniform in thickness, it is important to control the concentration of polymer, composition of solvent, amount of solution deposited, and the rate of evaporation of solvent (Taylor and Schultz, 1996). Moreover, good dispersion is obtained taking advantage of the common solvent effect (water) for the polymer phase and the reinforcing phase (e.g. CNC). It is also reported that slow rate of evaporation allows the formation of a two-dimensional network of nanocrystals in the matrix phase, which enhances the mechanical properties of biocomposite materials (Oksman et al., 2014).

2.7 Characterizations of PVA Blended Films

2.7.1 Tensile Test

As reported by Ramaraj (2006), the elastic modulus increased as the addition of coconut shell (CCS) powder increased whereas both the tensile strength and elongation at break decreased, which was showed in the stress-strain curves in Figure 2.7. Based on the curves, it was observed that PVA100 has the lowest value of elastic modulus, which was 4.15 N/ mm^2 and PVA50/CCS50 has the highest modulus of elasticity, which was 140.08 N/ mm^2. In contrast, PVA100 has the highest tensile strength and elongation at break which was 13.34 N/ mm^2 and 500%, respectively.

Similar results were reported by Ooi et al. (2012a) on PVA and rambutan waste flour (RWF) as well as banana waste flour (BWF) composite films. The increased in elastic modulus and the decreased in elongation at break were attributed to the weak agglomerations and non-uniform dispersion of the higher filler (CCS, RWF and BWF) contents in the PVA matrix in addition to the stiffening effect of filler and less effective cross-sectional area of the PVA towards filler. Hence, the presence of filler did not improve the tensile properties of PVA blended films because of the poor compatibility of PVA and filler, and the extremely good mechanical properties of PVA (Ooi et al., 2012a; Suki, Ismail and Hamid, 2014).

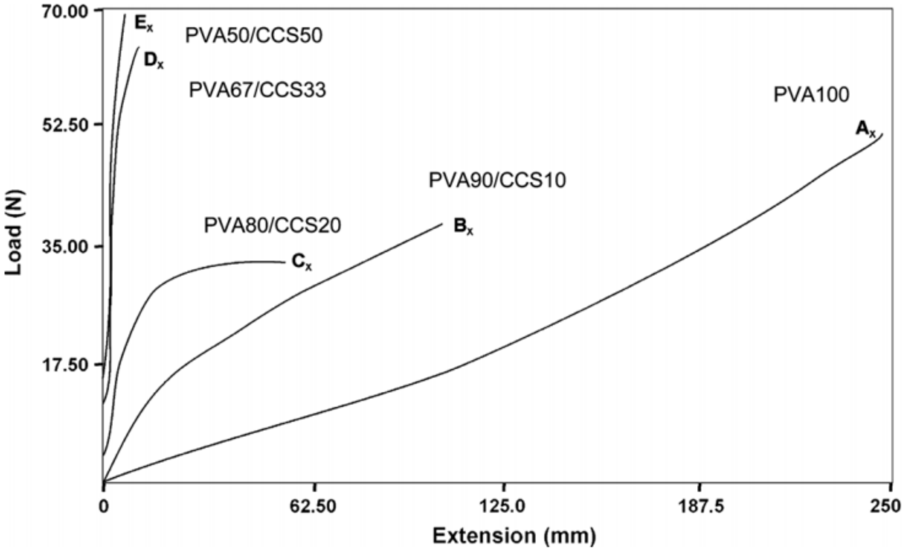

Figure 2.7: Stress-strain curves of PVA/CCS films (Ramaraj, 2006).

2.7.2 Natural Weathering Test

Natural weathering test is a test carried out to determine the durability of a material in a natural condition such as sunlight, UV radiation, rainfall, dew, moisture, humidity, etc. These environmental factors lead to embrittlement or catastrophic failure of the material, once exposed to outdoor weathering (Schiers, 2000). For instance, this test was performed for two weeks, where the dumbbell specimens were arranged on an exposure to look out on the equator at 45˚ inclination and placed in an exposed area, ensuring that the specimens were free from overshadowing by other objects. After the exposure duration, the specimens were taken for mechanical testing and SEM analysis (Suki, Ismail and Hamid, 2013).

The elastic modulus of PVA/RWF and PVA/BWF blend films increased after being exposed to the environment for one month, indicating that the films became stiffer due to the stiffening effect of the RWF and BWF. On the other hand, the tensile strength and elongation at break decreased due to surface cracking and degradation as a consequence of PVA chain scission when films were subjected to prolonged natural weathering such as rainfall and UV rays, respectively (Ooi et al., 2011b; Suki, Ismail and Hamid, 2013). Due to the hydrophilic nature of PVA and RWF, they tend to shrink when exposed to sunlight and swell when rain, which is referred to as annealing effect (Suki, Ismail and Hamid, 2013).

2.7.3 Field Emission Scanning Electron Microscope (FESEM) analysis

One of the major determinants of the properties of polymer blends is the morphology. As reported by Othman, Azahari and Ismail (2011), different weight ratio of poly(vinyl alcohol) (PVA)/ corn starch (CS) blend films were prepared by solution casting method and the surface morphology of the blended films was characterized using FESEM. According to Figure 2.8, corn starch granules have elliptical shape whereas the pure PVA contained voids which were attributed to the trapped bubble in the sample during the casting of the film. When the concentration of starch was increased, the corn starch phase reversed to be continued phase from the dispersed phase, which indicates that amorphous starch is partially miscible with PVA. Similar observations were reported by Zhou, Jin and Xin (2008) on the extruded starch/PVA composites.

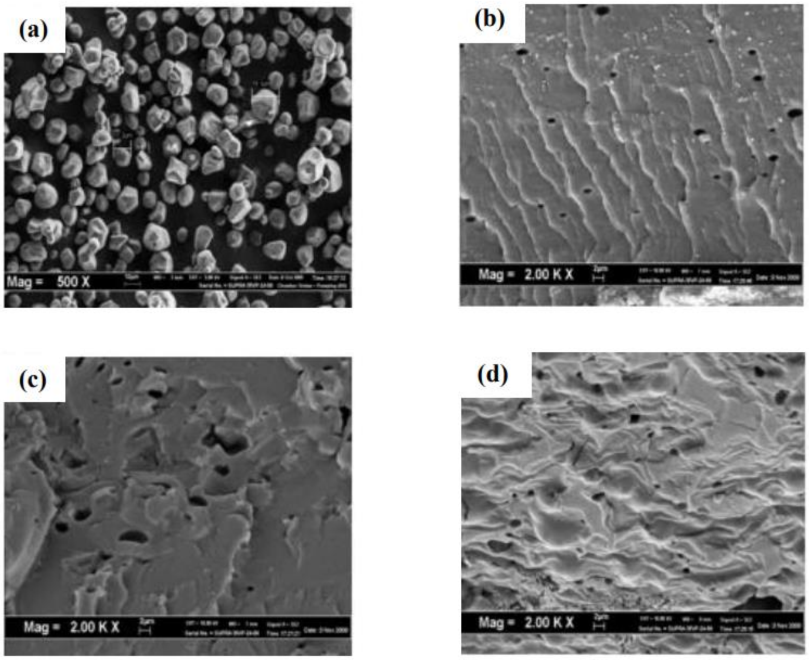

Figure 2.8: The surface morphology of PVA/CS blend films with weight ratio of (a) 0:100, (b) 100:0, (c) 70:30 and (d) 30:70 (Othman, Azahari and Ismail, 2011).

From the Figure 2.8 (c), corn starch was finely dispersed in the PVA matrix with the weight ratio of 70:30 but the addition of corn starch up to 70% caused the cryo-fractured surface to become rougher and more brittle. This is due to the coalescence of starch granules instantaneously although PVA was finely dispersed in the corn starch granules. Therefore, it can be concluded that the weight ratio of 70:30 PVA matrix has the best dispersion of starch granules (Othman, Azahari and Ismail, 2011).

CHAPTER 3

METHODOLOGY

3.1 Materials

Valencia oranges were purchased from Northridge International Sdn. Bhd., Batu Caves, Kuala Lumpur, Malaysia and the orange peels (OP) were collected and used in this research. The chemicals used in this research include ethanol and microcystalline cellulose purchased from Sime Scientific, toluene and glycerol purchased from Friendemann Schmidt, sodium hydroxide (NaOH) purchased from Merck (Germany), sodium chlorite ($NaClO_2$, 80%) purchased from Acros Organics (Spain), acetic acid glacial purchased from Bendosen, and poly(vinyl alcohol) (PVA) purchased from Sigma Aldrich (USA).

3.2 Equipment/ Instruments

The equipment or instruments used in this research are grinder (brand: model: RT-08), centrifuge machine (model: 416 G), Attenuated Total Reflectance Spectrophotometer (ATR) (brand: Perkin Elmer; model: Spectrum Two), Field Emission Scanning Electron Microscope (FESEM) (brand: JEOL Japan; model:

JSM 6701F), particle size analyzer (brand: Malvern; model: Masterizer (Hydro 2000 MU)), refractometer (brand: Lauda; model: Alpha RA δ), X-Ray Diffraction (XRD) (brand: Shimadzu; model: XRD 6000), thickness gauge (brand: Mitutoyo), dumbbell cutter, tensile tester (brand: Tinius Olsen; model: H10KS), and Differential Scanning Calorimetry (DSC) (brand: Mettler Toledo; model: DSC1).

3.3 Flow Chart of Research

The flow chart of research is portrayed in Figure 3.1, which shows the extraction, isolation and characterization of cellulose from OP and Figure 3.2, which shows the preparation and characterization of PVA/cellulose blended film.

3.4 Collection and Preparation of Orange Peels (OP)

The Valencia oranges purchased from Northridge International Sdn. Bhd., Batu Caves, Kuala Lumpur, Malaysia were peeled off and the OP were collected. The peels were cut into small pieces, washed clean with water and oven-dried at 80˚C for overnight. The dried OP was then grinded into powdered form using grinder and stored in a Schott bottle to avoid air moisture prior to further treatment and analysis.

3.5 Maceration of Orange Peels

The ground OP was macerated in ethanol/toluene solution for 3 days with the ratio 1:15. The extracted orange oil was removed and the ground OP was rinsed with distilled water. It was then centrifuged at 3500 rpm for 10 minutes to remove the solvent completely and the sample was dried in the oven at 50˚C overnight.

3.6 Extraction of Cellulose

The macerated OP was weighed and transferred into a round-bottomed flask. Alkaline treatment was performed by using 5% (w/v) sodium hydroxide (NaOH) with the ratio 1:15 heated at about 80˚C for 3 hours. The cellulose was centrifuged at 3500 rpm for 10 minutes and washed with distilled water for several times until a neutral pH was obtained. The cellulose was then subjected to bleach by using 1.7% (w/v) sodium chlorite solution ($NaClO_2$) with the ratio 1:15. It was acidified to pH 4 with the addition of acetic acid glacial and heated at about 80˚C for 2 hours. The mixture was cooled, centrifuged at 3500 rpm for 10 minutes and washed with distilled water until white cellulose was obtained. It was then dried in the oven at 50˚C for overnight. The percentage yield of orange peel derived cellulose (OPDC) was calculated by using Equation 3.1 as shown below.

$$\text{Yield}(\%) = \frac{\text{Mass of OPDC (g)}}{\text{Mass of macerated OP used (g)}} \times 100\% \qquad \text{(Equation 3.1)}$$

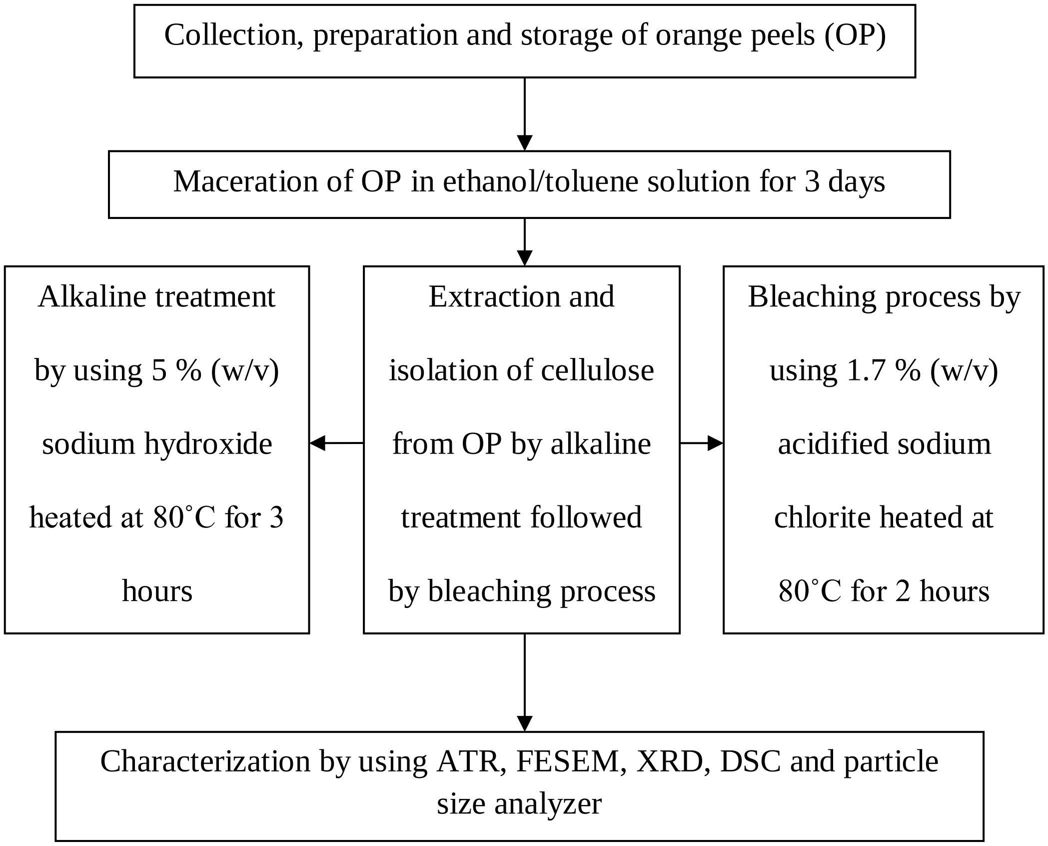

Figure 3.1: Extraction, isolation and characterization of cellulose from OP.

3.7 Characterization of Orange Peels (OP) and Orange Peel Derived Cellulose (OPDC) and Microcrystalline Cellulose (MCC)

The dried and ground OP, OPDC obtained from alkaline treatment with 5 % (w/v) sodium hydroxide (NaOH) and MCC was characterized using Attenuated Total Reflectance Spectrophotometer (ATR), Field Emission Scanning Electron

Microscope (FESEM), X-Ray Diffraction (XRD), Differential Scanning Calorimetry (DSC) and particle size analyzer.

3.7.1 Attenuated Total Reflectance Spectroscopy (ATR)

The ATR spectra for OP, OPDC and MCC were obtained by using ATR spectrophotometer (brand: Perkin Elmer; model: Spectrum Two) to determine the presence or absence of functional groups before and after treatment. An appropriate amount of sample (which was grinded homogenously beforehand) was placed on the diamond cell. The pressure controller was then screwed down until the pressure gauge on the software program shows the optimum level of pressure between 60 to 80%. The ATR spectra were analyzed in the wavenumber range from 400 to 4000 cm^{-1} with a resolution of 4 cm^{-1} for 32 scans.

3.7.2 Field Emission Scanning Electron Microscopy (FESEM)

JEOL Japan SEM, JSM 6701F was used to study the surface morphology and microstructure of the samples. The sample was deposited on the copper stub with the aids of carbon tapes and was left to dry in the oven at 50˚C for 20 minutes. The sample was sputter coated with thin layer platinum (thickness 15nm, density: 21.45 g/cm^3) by using sputtering machine (brand: JEOL; model: JFC-1600). This is to avoid the electrostatic charging and poor resolution during analysis. The image of the morphology of sample can be observed with magnification of×500, 1000, 2000, 10 000, 20 000 and 50 000 at 4.0 kV accelerating rate.

3.7.3 Particle Size Analysis

Particle size analyzer (brand: Malvern; model: Masterizer (Hydro 2000 MU)) was used to determine the size of the OPDC and MCC. Firstly, a refractometer (brand: Lauda; model: Alpha RA δ) was used to determine the refractive index of both OPDC and MCC. During analysis, distilled water was used as suspension medium for cellulose particles dispersion. Then, the probe of the particle size analyzer was immersed into the suspension for analysis.

3.7.4 Differential Scanning Calorimetry (DSC)

DSC (brand: Mettler Toledo; model: DSC1) with automatic voltage regulator was conducted to determine the thermal properties of OPDC and MCC. About 2-3 mg of sample was weighed and sealed into an aluminium crucible. An empty aluminium crucible was used as reference cell. DSC analysis was carried out at a heating rate of 10˚C/min from 25˚C to 280˚C with two heating and one cooling scan in nitrogen atmosphere.

3.7.5 X-Ray Diffraction (XRD)

OP, OPDC and MCC were analyzed using XRD to determine the crystallinity of cellulose. A Shimadzu XRD 6000 X-ray diffractometer operating at 40 kV and 30 mA was used to obtain the diffraction profile at 2˚C per min. Samples were scanned using a monochromatic Cu-Kα radiation source (λ = 1.5406 Å) in the step-scan mode with a 2θ angle ranging from 5˚ to 70˚.The crystallinity index, CrIor the degree of crystallinity was determined by Segal method using the Equation 3.2 as outlined by Chieng et al. (2017), where I_{002} provides the maximum peak intensity value for the crystalline cellulose at about 2θ = 22.0˚ to 24˚ and I_{am} gives the peak intensity of diffraction of the amorphous region at about 2θ = 18.0˚ for cellulose type I (Szymańska-Chargot et al., 2017; Hussin et al., 2018).

$$\%CrI = \frac{I_{002} - I_{am}}{I_{002}} \times 100 \qquad \text{(Equation 3.2)}$$

3.8 Preparation of PVA/OPDC and PVA/MCC Blended Films

Total of 2% (w/v) of varying composition of PVA/OPDC and PVA/MCC blended films were prepared. In a 50 mL beaker, the cellulose was dispersed in distilled water and stirred at 35˚C for 30 minutes. Glycerol was then added into the solution and stirred for another 30 minutes. At the same time, PVA solution was stirred at about 90˚C for 1 hour in a separate beaker. Then, the cellulose suspension was added into the PVA solution and stirred for another 1 hour. After that, the PVA/cellulose solution was poured onto the petri dish to cast the blended film. The blended film was air dried for overnight and then dried in the oven at 50˚C for 2days. The above procedures were repeated to cast different compositions of PVA/cellulose blended films with the ratio 2.0:0, 1.5:0.5, 0.5:1.5 and 0:2.0. Lastly, the films were kept in the desiccator prior to further analysis.

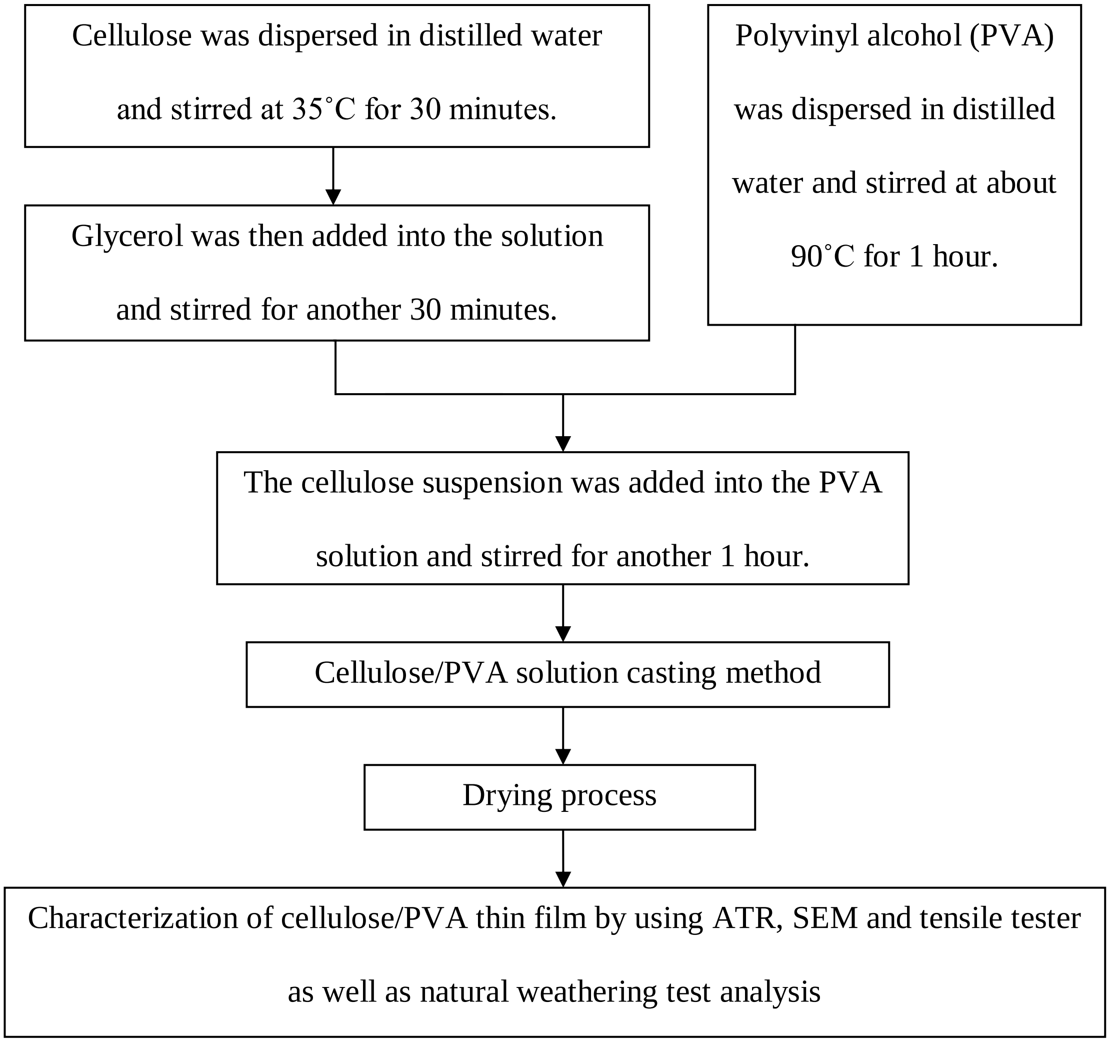

Figure 3.2: Preparation and characterization of PVA/cellulose blended film.

3.9 Characterization of PVA/OPDC and PVA/MCC Blended Films

Characterization of the different compositions of 2 % (w/v) of PVA/OPDC and PVA/MCC blended films were carried out such as Attenuated Total Reflectance (ATR) Spectroscopy, Field Emission Scanning Electron Microscopy (FESEM), tensile test and natural weathering test.

3.9.1 Attenuated Total Reflectance Spectroscopy (ATR)

The ATR spectra for PVA/OPDC and PVA/MCC blended films were obtained by using ATR spectrophotometer (brand: Perkin Elmer; model: Spectrum Two) to determine the presence or absence of functional groups before and after treatment and the change in intensity of the peaks. An appropriate amount of blended film was placed on the diamond cell. The pressure controller was then screwed down until the pressure gauge on the software program shows the optimum level of pressure between 60 to 80%. The ATR spectra were analyzed in the wavenumber range from 400 to 4000 cm^{-1} with a resolution of 4 cm^{-1} for 32 scans.

3.9.2 Tensile Properties

The tensile strength and elongation at break of the composite films was measured on the Tinius Olsen H10KS tensile tester by applying 450 N load range on the film with a speed of 10 mm/min. A dumbbell cutter was used to cut the film with gauge length of 26 mm and width of 3 mm. Then, the thickness gauge (brand: Mitutoyo) was used to measure the thickness of the film by taking the reading at three points to obtain the average value. Average value was obtained by measuring five specimens for each composite film.

3.9.3 Natural Weathering Test

The aim of natural weathering test is to determine the biodegradability of film. The film was cut into smaller rectangular shape with approximately the same dimensions for each composition of the film. The film was dried overnight and weighed before exposed to the environment. This test was carried out for a month and the weight loss of the film was measured every week using a weighing balance. Equation 3.3 shows the calculation for percentage of film degradation.

$$\text{Percentage of degradation}(\%) = \frac{\text{Initial weight (g)} - \text{final weight (g)}}{\text{Initial weight (g)}} \times 100\%$$

(Equation 3.3)

3.9.4 Morphology Studies of Degraded Films by Field Emission Scanning Electron Microscopy (FESEM)

The surface morphology of the degraded film was studied using FESEM (brand: JEOL Japan SEM; model: JSM 6701F) to determine the growth of microbes on the film. The sample was attached on the aluminium stub with the aids of carbon tapes.

The sample was sputter coated with thin layer platinum (thickness 15nm, density: 21.45 g/cm^3) by using sputtering machine (brand: JEOL; model: JFC-1600). The image of the morphology of sample can be observed with magnification of ×500, 1000 and 2000 at 4.0 kV accelerating rate.

CHAPTER 4

RESULTS AND DISCUSSIONS

4.1 Extraction of Cellulose from Orange Peels (OP)

4.1.1 Physical Appearances of Orange Peels (OP) Before and After Chemical Treatment Processes

Figure 4.1 shows the physical appearances of OP, grinded OP, alkaline treated OP, bleached OP suspension and dried OPDC. The changes in appearances of OP during the maceration process were shown in Figure 4.2. After soaking the grinded OP in ethanol/toluene solution (Figure 4.2 (a)) for three days, the OP turned from orange colour to light yellow and a layer of wax and oils was formed as shown in Figure 4.2 (b). This is an indication of the removal of hydrophilic compounds such as pigments cellular debris by ethanol and extraction of wax and oils by toluene. According to Figure 4.2 (c), the clear solution indicates the complete removal of solvents by washing the OP with distilled water for several times and the light yellow OP suggests that organic solvent extraction also reduces the colouring of the OP (Naz et al., 2016).

Figure 4.3 shows the colour changes of OP during alkaline treatment. When the OP was treated with sodium hydroxide solution, the mixture was dark brown in colour. When the OP was subjected to second alkaline treatment, the mixture turned from dark brown to light orange followed by pale yellow in the third alkaline treatment. The changing in the colour of the mixture indicates the removal of hemicellulose and lignin. Moreover, the size and diameter of the OP fibres were reduced after the third alkaline treatment was carried out (Chieng et al., 2017; Ilyas, Sapuan and Ishak, 2018). Lignin was removed from the OP in large amount during the bleaching treatment by acidified sodium chlorite, which can be proved by the produced suspension that was white in colour as shown in Figure 4.1 (d) (Pelissari, do Amaral Sobral and Menegalli, 2014; Berglund et al., 2016).

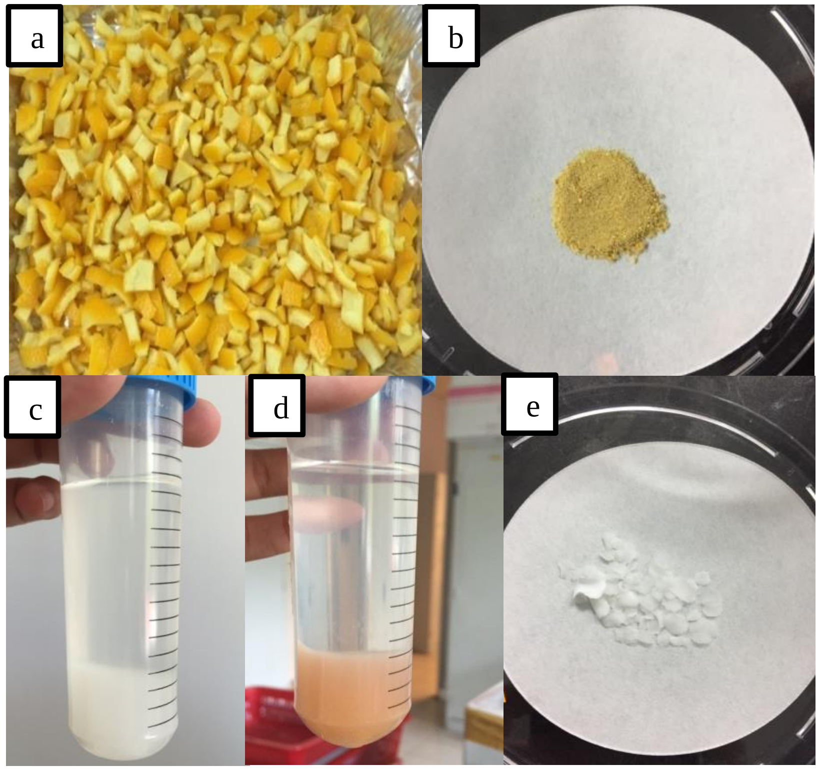

Figure 4.1: Physical appearances of (a) OP, (b) grinded OP, (c) alkaline treated OP, (d) bleached OP suspension and (e) dried OPDC.

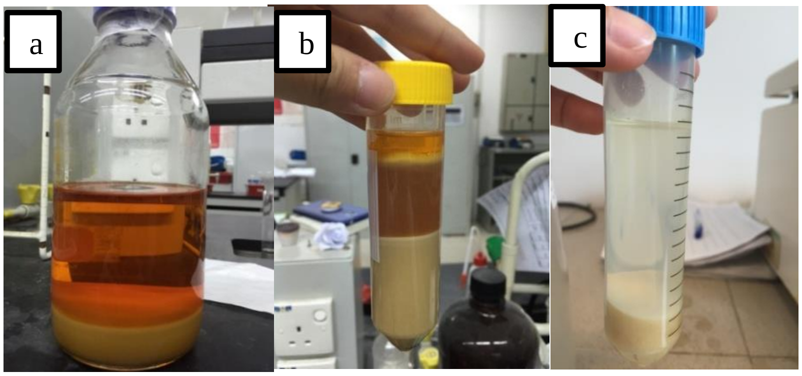

Figure 4.2: Physical appearances of (a) OP in ethanol/toluene solution, (b) formation of a layer of wax and oils and (c) solvent-free OP.

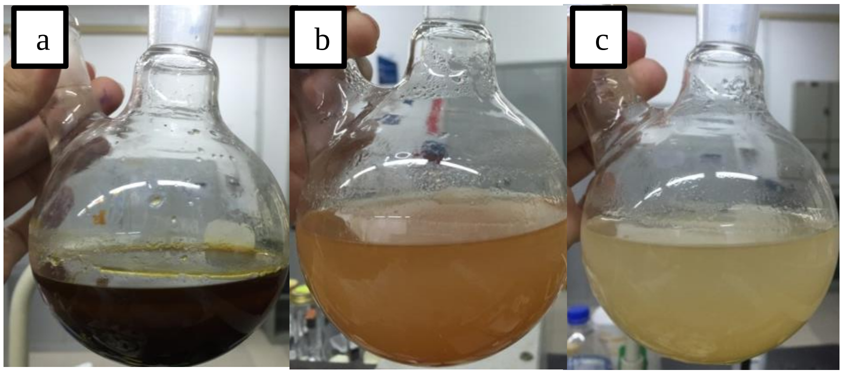

Figure 4.3: Colour changes of OP during (a) first, (b) second and (c) third alkaline treatment.

4.1.2 Percentage Yield of the Orange Peel Derived Cellulose (OPDC)

Table 4.1 shows the average percentage yield of OPDC after alkaline and bleaching treatment, which was calculated using Equation 3.1. According to Abraham et al.

(2011) and Ilyas, Sapuan and Ishak (2018), the weight loss was an indication of the removal of hemicellulose, lignin, pectin, fat, impurities, wax and oils from the OPDC, which contributes to the very low percentage yield of OPDC. The weight loss also occurred as the alkaline treatment was carried out for three times to obtain a higher purity of the OPDC.

Table 4.1: Percentage yield of OPDC.

No.	Mass of OP used (g)	Mass of cellulose obtained (g)	Percentage yield (%)
1	6.6677	1.3339	20.01
2	6.6677	1.3500	20.25
3	6.6693	1.3577	20.36
4	6.6667	1.3638	20.46
5	6.6732	1.3549	20.30
Average			20.28

4.2 Characterization of Orange Peels (OP), Orange Peel Derived Cellulose (OPDC) and Microcrystalline Cellulose (MCC)

4.2.1 Attenuated Total Reflectance Spectrophotometer (ATR)

ATR spectroscopy was used to determine the presence or absence of functional groups before and after treatment. Figure 4.4 shows the ATR spectra of OP, OPDC and microcrystalline cellulose (MCC) and Table 4.2 shows the summary of ATR spectra of OP, OPDC and MCC. The ATR spectra of OPDC were compared with reference sample (MCC). The appearance of peaks on the spectra of OPDC corresponds to bands of MCC, while differences in absorption peaks intensities and presence of new peaks in spectra of OP are observed. The broad absorption bands around 3200 – 3300 cm^{-1} region indicate the hydrogen bond O – H stretching vibration whereas the absorption peaks around 1600 – 1640 cm^{-1} were the O – H bending of absorbed water. The absorption peaks near 2900 cm^{-1} correspond to aliphatic C – H stretching vibration of all hydrocarbon constituent in polysaccharides (Lu and Hsieh, 2010; Hospodarova, Singovszka and Stevulova, 2018). The intensity of the C-H stretching peak of OPDC and MCC was slightly lower than OP, which indicates that both of the lignin and hemicellulose were removed from the OPDC during the bleaching process (Yang, et al., 2007; Lani, et al., 2014).

One distinguishable vibration peak can be seen at 1736 cm^{-1} on the OP, which can be ascribed to the presence of the C=O stretching vibration of the acetyl group of hemicelluloses. The disappearance of this peak on the OPDC as well as MCC was due to the removal of hemicelluloses after treatment with sodium hydroxide, NaOH (Liu et al., 2004; Sgriccia, Hawley and Misra, 2008; Zarina and Ahmad, 2014; Luo and Wang, 2017). Next, the absorption peak at 1236 cm^{-1}, which indicates the C – O stretching of the aryl group of lignin has disappeared on the spectra of OPDC and MCC. This portrays the partial removal of lignin from the OP surface (Liu et al., 2004; Sgriccia, Hawley and Misra, 2008). The absence of the two peaks in the spectra of OPDC and MCC indicates that alkaline treatment has removed most of the lignin and hemicellulose found in OP (Zarina and Ahmad, 2014). Furthermore, the peaks in the regions around 1160 cm^{-1} was assigned to C – O – C asymmetrical ring stretching (Fan, Dai and Huang, 2012; Zarina and Ahmad, 2014) while the peaks in the regions around 1012 – 1039 cm^{-1} are contributed by the C – O – C bending of pyranose ring in the cellulose (Lani, et al., 2014). Lastly, the peaks found on both OPDC and MCC spectra at 1425 – 1428 cm^{-1} indicates the CH_2 symmetric bending while the peak at 896 cm^{-1}are contributed by the stretching of the β-glycosidic linkages between the cellulose (Fan, Dai and Huang, 2012).

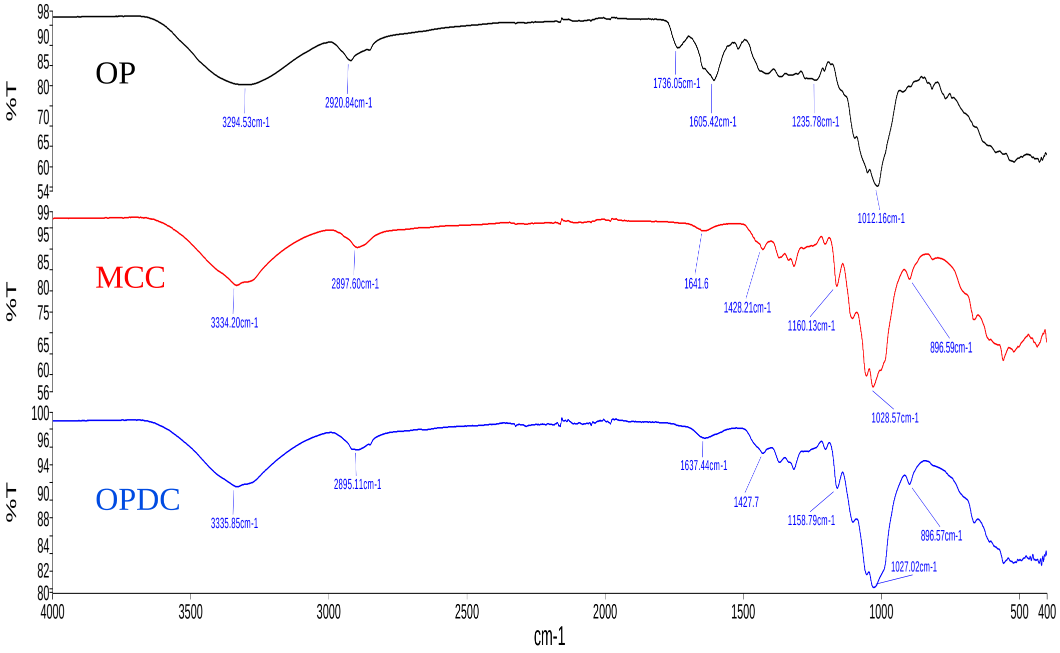

Figure 4.4: ATR spectra of OP, MCC and OPDC.

Table 4.2: Summary of ATR spectra of OP, MCC and OPDC.

Types of stretching or bending	**Wavenumber (cm^{-1})**		
	OP	**OPDC**	**CMC**
O-H stretching	3295	3336	3334
Aliphatic saturated C-H stretching	2921	2895	2898
C-O stretching (aryl group)	1236	-	-
O-H bending of absorbed water	1605	1639	1637
C=O stretching	1736	-	-
C-O-C asymmetrical ring stretching	-	1159	1160
C-O-C bending (pyranose ring)	1012	1027	1029
β-glycosidic linkages between glucose	-	897	897
CH_2 symmetric bending	-	1428	1428

4.2.2 Field Emission Scanning Electron Microscopy (FESEM)

Figures 4.5 and 4.6 show the surface morphologies of untreated OP and OPDC, respectively. The untreated OP revealed non-uniform surface with irregular shape of many non-cellulosic materials such as the gummy polysaccharides of hemicellulose, lignin, pectin and waxes are scattered over the surface (Reddy and Yang, 2009; Liu et al., 2013; Mzimela et al., 2018). The surface was smooth and the orientation of cellulose microfibril aggregates was not prominent however can be clearly observed in OPDC shown in Figure 4.6 (Chen et al., 2017). In addition, the delignified OPDC with cleaner surface indicates the removal of lignin and other extractives such as waxes, oil and pectin after delignification process using acidified sodium chlorite. The uniform distribution of micrfibrillated cellulose shown in Figure 4.6 also revealed the removal of hemicellulose found in the OP by alkaline treatment (Kumar et al., 2014).

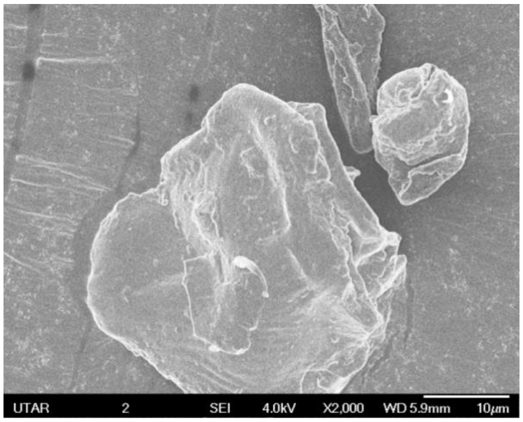

Figure 4.5: FESEM image of the surface morphology of untreated OP with the magnifying power of ×2000.

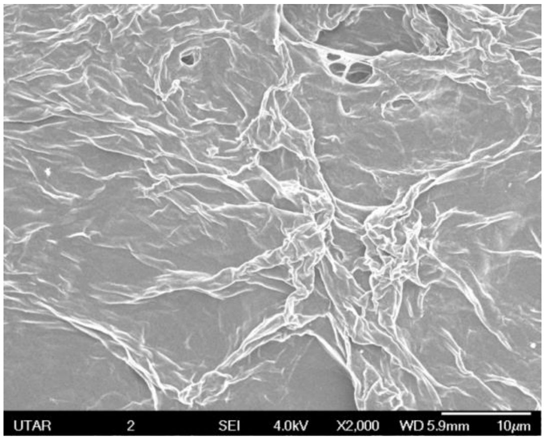

Figure 4.6: FESEM imageof the surface morphology of OPDC with the magnifying power of ×2000.

4.2.3 Particle Size Analysis

The particle size distribution of cellulose was determined using particle size analyser (brand: Malvern; model: Masterizer (Hydro 2000 MU)). The refractive index of both OPDC and MCC was determined using a refractometer (brand: Lauda; model: Alpha RA δ) prior to the particle size measurement. The refractive index of OPDC measured was 1.33 and the same goes to MCC. Figures 4.7 and 4.8 show the particle size distribution of OPDC and MCC, respectively. According to Figure 4.7, 11% of the total amount of OPDC particles was distributed in the range of 0.060 to 0.091μm. On the contrary, Figure 4.8 shows the particle size distribution of MCC in the range of 0.069 to 0.105 μm, which contributed up to 13% of the total amount of particles. The results of study revealed that the OPDC has become micro-sized after treatment with alkaline, with the OPDC having smaller average particle size of 0.076 μm as compared to that of MCC (0.088 μm).

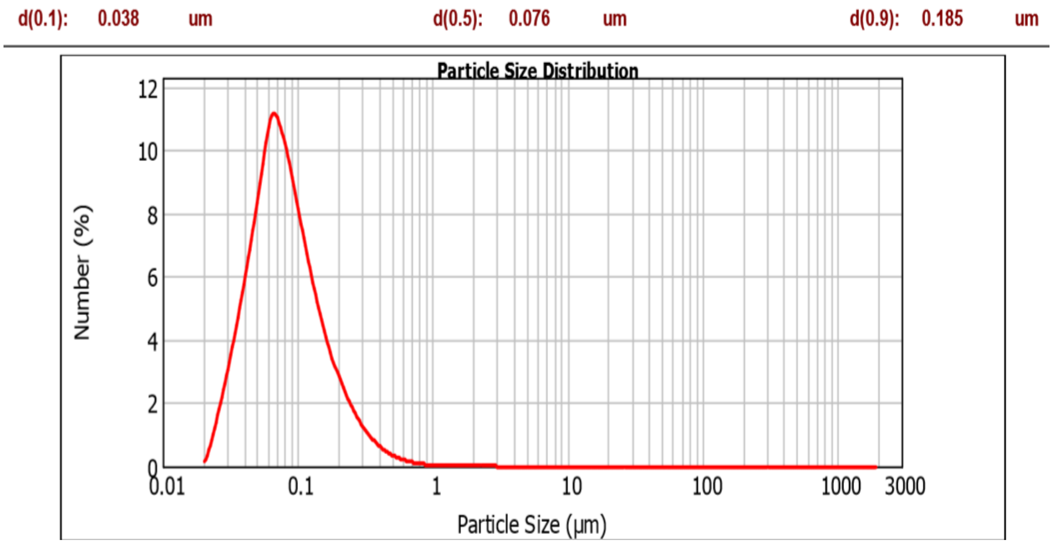

Figure 4.7: Particle size distribution of OPDC.

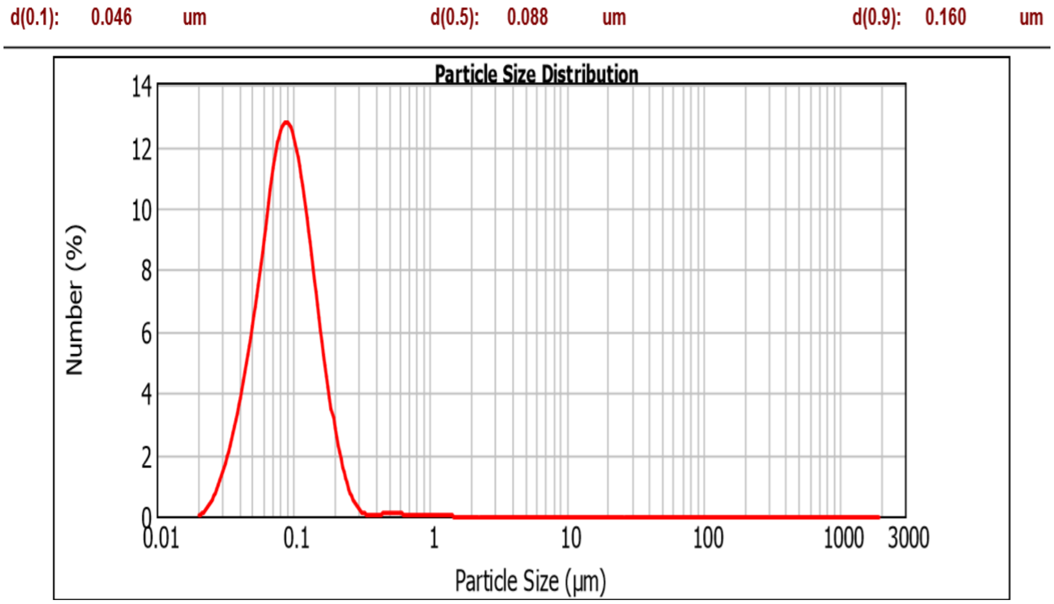

Figure 4.8: Particle size distribution of MCC.

4.2.4 Differential Scanning Calorimetry (DSC)

DSC test was carried out for OPDC with comparison to MCC as a reference material. Figure 4.9 and 4.10 shows the thermal behaviour of OPDC and MCC. By comparing the graphs, the value of melting temperature, T_m for MCC (176˚C) was higher than that of MCC (170˚C) due to the elimination of hemicellulose after acid hydrolysis of the MCC (Kuthi, Norzali and Badri, 2016; Hussin et al., 2018).

MCC are showing a slight peak around 125˚C which could indicate the cold crystallization temperature, T_{cc}. This could be explained by the nucleation crystallization of MCC molecules. According to literature, cold crystallization peaks show areas of realignment and transition from amorphous to crystalline phases. However, the peak around 125˚C may not be a peak but rather appeared due to noise. Therefore, the peak was not regarded as an indication for crystallinity (Sumigin et al., 2012; Taib, Ghaleb and Mohd Ishak, 2012). Lastly, the higher onset temperatures were often attributed to higher thermal stability. Hence, MCC has higher thermal stability and is more widely applicable in food stabilizers, biocomposites and pharmaceutical compounds (Hussin et al., 2018).

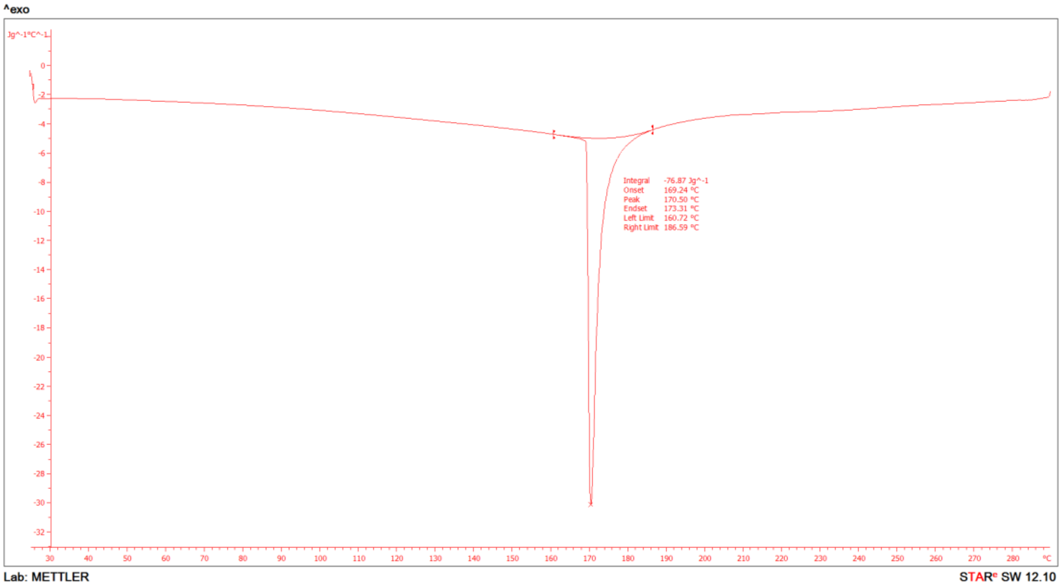

Figure 4.9: DSC curve of OPDC.

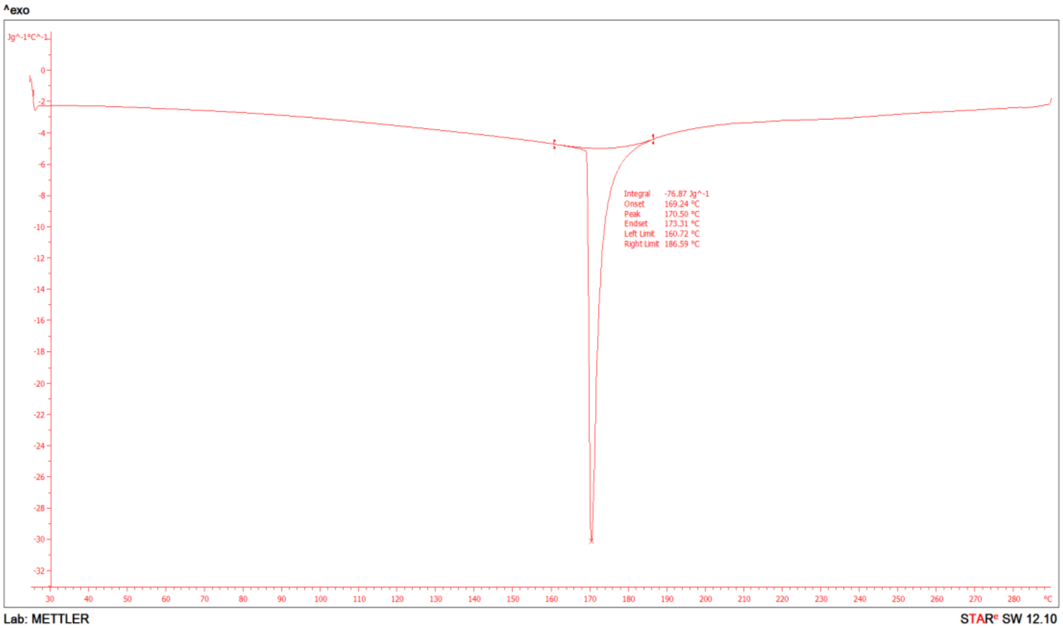

Figure 4.10: DSC curve of MCC.

4.2.5 X-Ray Diffraction (XRD)

XRD analysis was carried out to determine the crystallinity index in addition to the changes of the crystallinity and amorphous region of untreated OP and OPDC after treatment in comparison with the commercial cellulose (MCC) (Zain, Yusop and Ahmad, 2014). According to Chieng et al. (2017), crystallinity index is the ratio of the crystalline to the amorphous regions of cellulose. Figure 4.11 shows the XRD curves of OP, OPDC and MCC and Table 4.3 shows the crystallinity indexes of the different samples.

Untreated OP has the lowest percentage of crystallinity, which was 23.54% as it has high amount of amorphous region. However, there was an increased in crystallinity of the OPDC (80.14%) after treatments via alkaline and bleaching due to the removal of hemicellulose and lignin, which exist in the amorphous phase. By comparison, it was clearly observed that the diffraction peak of OPDC becomes sharper than the OP (Hussin et al., 2018), which corresponds to the increase in crystallinity. Cellulose derived from OP was confirmed by the high and sharp peak intensity located at a 2θ value of 22˚, which is the common value of cellulose type I. On the contrary, the amorphous phase of cellulose type I was characterized by the low diffracted intensity at a 2θ value of around 18˚ (Zain, Yusop and Ahmad, 2014).

The crystallinity index as calculated for MCC (87.69%) was slightly higher than that of OPDC (80.14%). In addition, the peak intensity of MCC located at a 2θ value of 22˚ was sharper than OPDC, which indicates that MCC is more crystalline than OPDC. According to Wan, Wang and Xiao (2010), the residual hemicellulose in α-cellulose, which is more amorphous compared to cellulose undergoes breakdown. Cellulose extraction by treatment with alkaline solution removes the major quantity of lignin, whereas the acid hydrolysis process used to produce MCC eliminates the residual amount of the amorphous lignin.

As reported by the researches, as a consequence of acid hydrolysis, most of the residual hemicelluloses were dissolved and lignin-hemicellulose-cellulose interactions were disrupted (Trache et al., 2014; Hussin et al., 2018). For instance, during the hydrolysis process, sulphuric acid attacks and invades the amorphous region of cellulose, which causes the hydrolytic cleavage of glycosidic bonds and consequently releasing individual crystallites. At the same time, growth and realignment of monocrystals may occur, leading to the increase in crystallinity of cellulose and giving a sharp diffraction peaks as shown in the XRD curve for MCC. In general, both of the OPDC and MCC samples possessed a high peak intensity of 2θ angle at 22˚, which was attributed to their crystalline structure of cellulose, whereas the presence of broad peak at around 15˚ indicates the amorphous arrangement. Hence, cellulose obtained from OP can be said as having cellulose type I structure (Chieng et al., 2017; Choi et al., 2018).

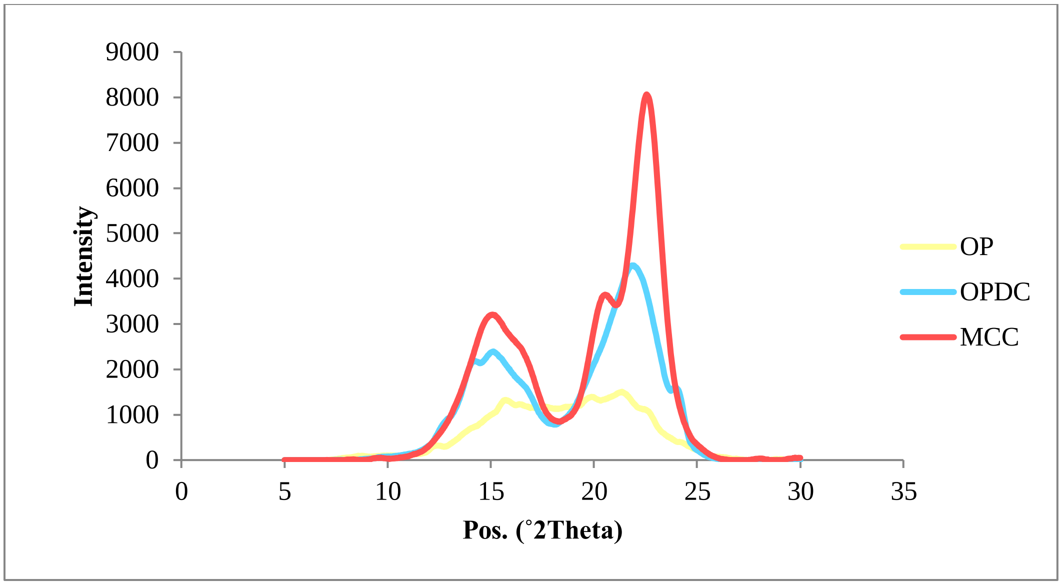

Figure 4.11: X-Ray Diffraction curves of OP, OPDC and MCC.

Table 4.3: Crystallinity index, CrI (%) of OP, OPDC and MCC.

Samples	**2θ (Amorphous) (◦)**		**2θ (Amorphous) (◦)**		**CrI (%)**
	Degree	**Intensity (I_{am})**	**Degree**	**Intensity (I_{002})**	
OP	17.82	1153	21.26	1508	23.54
OPDC	17.68	853	21.66	4294	80.14
MCC	17.78	993	22.45	8064	87.69

4.3 Physical Appearances of PVA/OPDC and PVA/MCC Blended Films

PVA/OPDC blended films with different loadings of OPDC were prepared by mixing of PVA water solution and OPDC suspension, followed by solution casting and controlled water evaporation. The same steps were repeated during the preparation of PVA/MCC blended films. The physical appearances of PVA/OPDC and PVA/CMC blended films at different compositions were shown in Figure 4.12 and Figure 4.13, respectively. When OPDC was dispersed in water, OPDC formed a very stable white cloudy suspension due to the strong hydrophilic characteristics of cellulose. When PVA and OPDC were added together, a more viscous suspension was formed due to the high affinity of PVA to bind the OPDC through hydrogen bonding. The same concept can be applied to MCC (Lu, Wang and Drzal, 2008; Frone et al., 2015).

It was observed that unfilled PVA film has high transparency while the transparency of PVA/OPDC and PVA/MCC blended films was diminished and a white colour film was formed when the amount of cellulose added was increased. Moreover, there was a decrease in homogeneity of the cellulose distribution starting from PVA/OPDC blended films with ratio of 0.5:1.5 (Figure 4.12 (c)) and PVA/MCC blended films with ratio of 1.0:1.0 (Figure 4.13 (c)). Hence, the transparency of the blended films confirms the uniform and homogenous dispersion of cellulose (OPDC and MCC) in PVA (Lu, Wang and Drzal, 2008). All films could be easily peeled from the petri dish due to the addition of glycerol, which provides flexibility and helps to soften the PVA blended films (Ooi et al, 2012a and 2012b) except the PVA/MCC blended films with ratio of 0.5:1.5 (Figure 4.14 (a)) and 0:2.0 (Figure 4.14 (b)). This is because MCC has a highly crystalline structure and hydrogen bonds. Hence, it could not form a film in its natural state as the amount of MCC added into the PVA increases.

On the contrary, PVA/OPDC blended films with ratio of 0.5:1.5 and 0:2.0 did not encounter this problem as modification of cellulose has been carried out during the alkaline treatment to transform it into water-soluble materials, also known as cellulose derivatives. However, shrinkage of the PVA/OPDC blended films took place with ratio of 0.5:1.5 (Figure 4.12 (c)) and 0:2.0 (Figure 4.12 (d)). According to literature, cellulose derivative films have poor water vapour barrier properties because of the hydrophilic nature of polysaccharides. Since the resistance to water vapour is poor, the films absorb water and shrink (Khalil et al., 2017). The appearance of both sides of the films were different, where the film side facing the petri dish was shiny and smooth while the other side was dull. This may be due to the polymer arrangement during water evaporation (Chen et al., 2018).

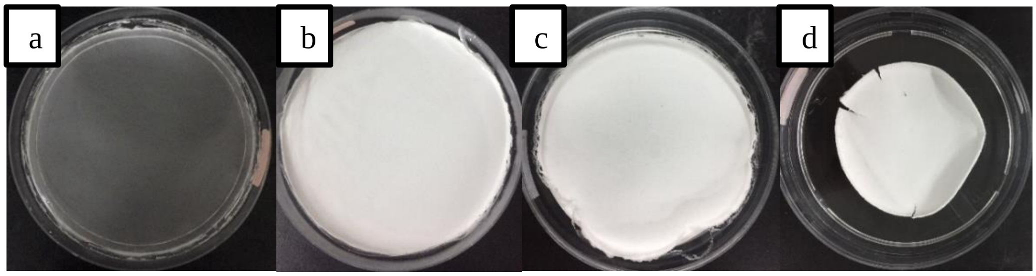

Figure 4.12: PVA/OPDC blended film with the composition of (a) 1.5:0.5, (b) 1.0:1.0, (c) 0.5:1.5 and (d) 0:2.0.

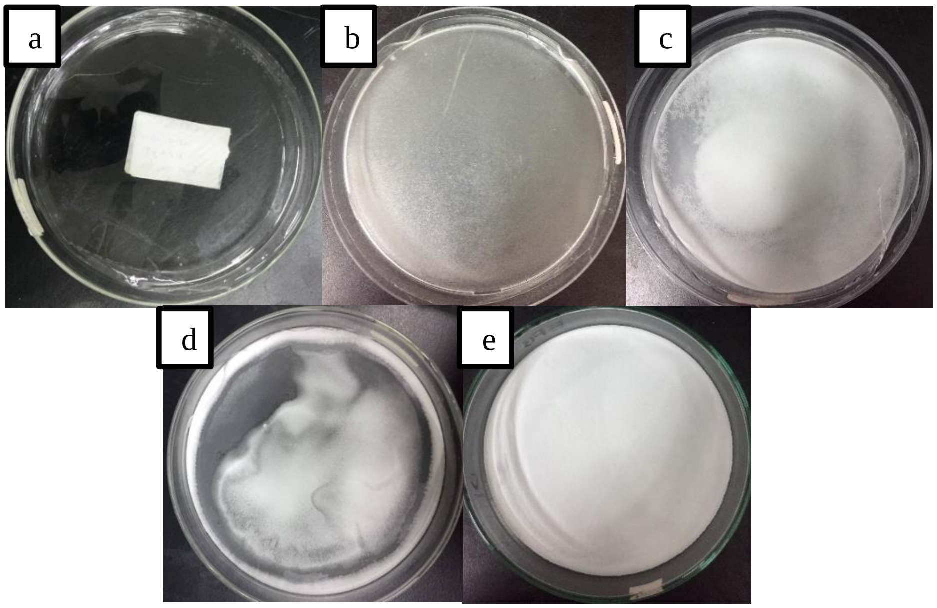

Figure 4.13: PVA/MCC blended film with the composition of (a) 2.0:0, (b) 1.5:0.5, (c) 1.0:1.0, (d) 0.5:1.5 and (e) 0:2.0.

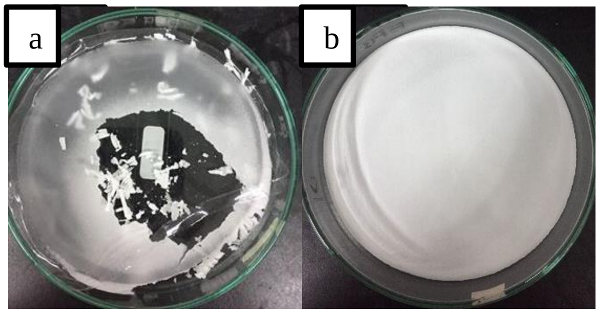

Figure 4.14: (a) The ruptured PVA/MCC blended film with the composition of 0.5:1.5 and (b) the powdered form of PVA/MCC blended film with the composition of 0:2.0.

4.4 Characterization of PVA/OPDC and PVA/MCC Blended Films

4.4.1 Attenuated Total Reflectance Spectroscopy (ATR)

Figure 4.15 shows the ATR spectra of unfilled PVA film and PVA/OPDC blended whereas Table 4.4 shows the summary of ATR spectra of unfilled PVA film and PVA/OPDC blended films. Figure 4.16 shows the ATR spectra of unfilled PVA film and PVA/MCC blended films whereas Table 4.5 shows the summary of ATR spectra of unfilled PVA film and PVA/MCC blended films. It was observed that the spectra of each of the blended film (PVA/OPDC and PVA/MCC) were similar to the spectra of unfilled PVA film. The shift of the characteristic absorption band and the change in intensity of the band observed in the spectra of PVA/OPDC blended films were similar to that of PVA/MCC blended films. This can confirm the development of new inter- and intramolecular hydrogen bonds and a change in the conformation between PVA and cellulose (Rahman, Afrin and Haque, 2014).

A band at 3272 cm^{-1} indicates the O – H stretching vibration of hydroxyl group of PVA. The addition of OPDC into the PVA solution caused a slight decrease of the intensity of O – H stretching in the regions around 3272 – 3289 cm^{-1}on the spectra of PVA/OPDC blend films, which can be ascribed to the interface between the hydroxyl groups on the surface of OPDC and the hydroxyl group in PVA (Choo et al., 2016; Siddaiah et al., 2018). Similar behavior was reported by Attia and El – Kader (2013) on PVA/2HEC polyblend films.

However, the PVA/MCC blended films (1.5:0.5 weight ratio) and PVA/MCC blended films (1.0:1.0 weight ratio) showed the peaks at 3272 $cm^{-1}$and 3282cm^{-1}, respectively, shifting the peaks to higher wavenumbers, therefore indicating that there were poor interactions of different OH groups between PVA and MCC during the process of blending and casting of the solution (Sudhamani, Prasad and Sankar, 2003; Ooi et al., 2011a). There was no absorption peak detected at 3600 cm^{-1}, which indicates that there was no free hydroxyl groups present in unfilled PVA film, PVA/OPDC and PVA/MCC blended films (Ibrahim, El-Zawawy and Nassar, 2010; Lu and Hsieh, 2010).

In addition, the absorption peak at 2909 cm^{-1} on the spectrum of unfilled PVA film, which corresponds to the aliphatic saturated C – H stretching has shifted towards higher stretching frequency observed in the regions around 2910 – 2913 cm^{-1} in the blended films. It can also be seen that the intensity of the peaks increased with increasing PVA content in the blended films (Fan, Dai and Huang, 2012; Choo et al., 2016; Siddaiah et al., 2018). Next, the absorption peaks around 1648 – 1658 cm^{-1} were the O – H bending of adsorbed water (Ibrahim, El-Zawawy and Nassar, 2010; Sarwar et al., 2018). Moreover, the absorption peak at 1417 cm^{-1} on the spectrum of unfilled PVA film indicates the CH_2 symmetric bending vibration. This band is also known as the "crystallinity band". In the spectra of PVA/OPDC and PVA/MCC blended films, there was a decreased in peak intensity, which reflects the decrease in the degree of crystallinity of PVA (Ciolacu, Ciolacu and Popa, 2011).

According to literature, the peaks in the regions around 1032 – 1044 cm^{-1}were contributed by the C – O – C bending of pyranose ring in the cellulose (Lani, et al., 2014), which indicates an increase in intermolecular bonding within the C – O in the C – O – C groups. It was also reported that the absorption band shifted to a lower wavenumber, which reflects an increase in intermolecular hydrogen bonding (Tang et al., 2008; Ooi et al., 2012a).

Lastly, the absorption peak around 900 cm^{-1} were contributed by the C – O – C stretching of the β-glycosidic linkages between the cellulose (Fan, Dai and Huang, 2012). Siddaiah et al. (2018) reported that the small absorption band at around 918 cm^{-1} was attributed to the characteristic of syndiotactic structure of the films due to the syndiotacticity of PVA, which caused dense molecular packing in the crystal and stronger intermolecular hydrogen bonds. This in turn led to the disappearance of the molecular motion.

As reported by the researches, the similarity of the shape and location of the characteristic peaks between unfilled PVA film and blended films (PVA/OPDC and PVA/MCC) suggests that the interactions among PVA molecules were dominated and were stronger as compared to those of PVA-OPDC molecules and PVA-MCC molecules in the blending system (Chen et al., 2008; Ooi et al., 2011a).

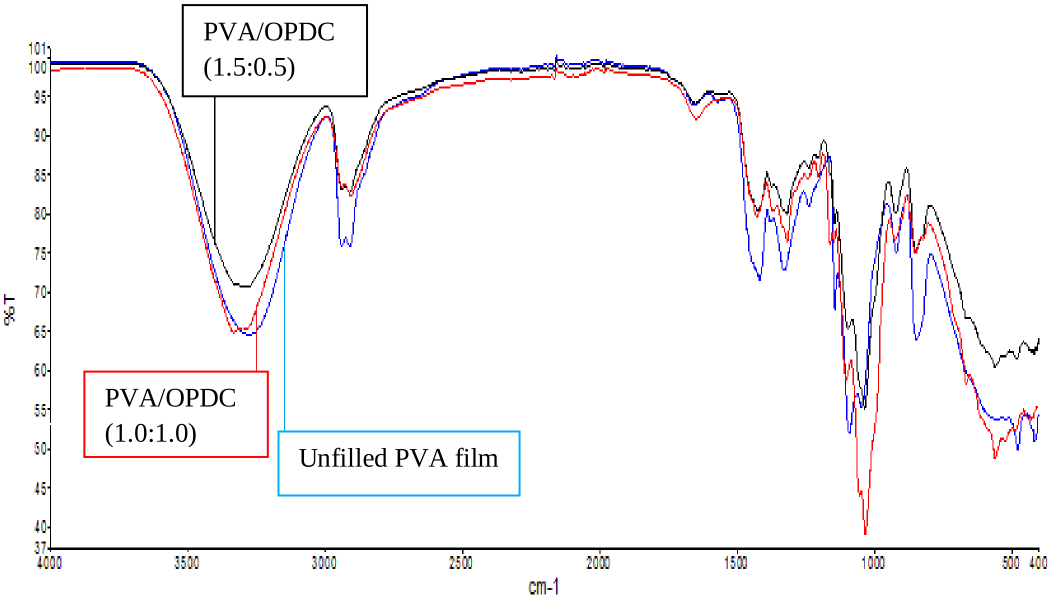

Figure 4.15: ATR spectra of unfilled PVA film and PVA/OPDC blended films.

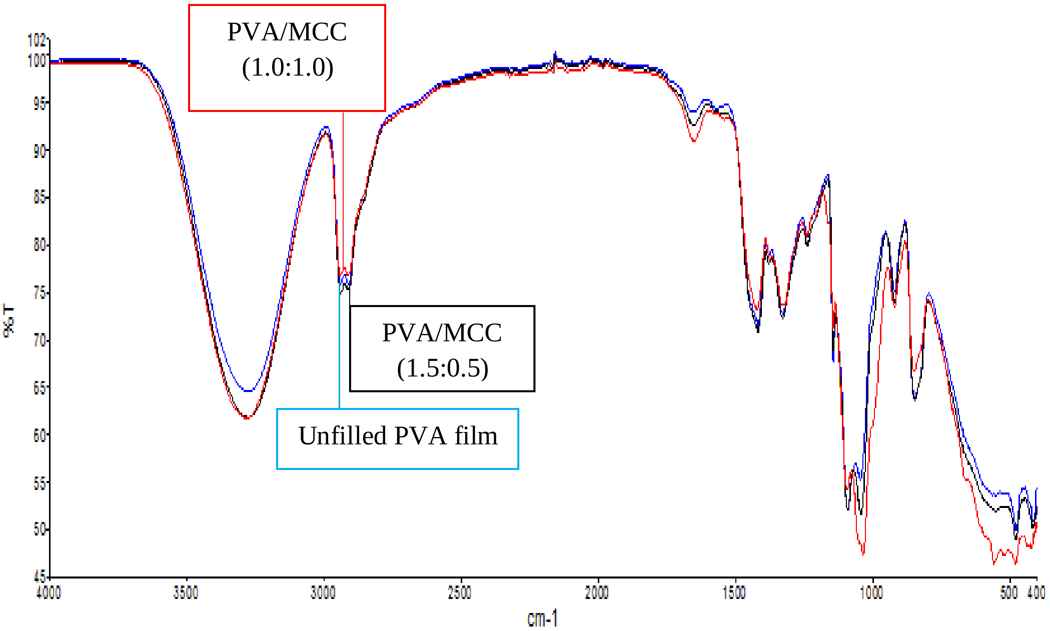

Figure 4.16: ATR spectra of unfilled PVA film and PVA/MCC blended films.

Table 4.4: Summary of ATR spectra of unfilled PVA film and PVA/OPDC blended films.

Types of stretching or bending	**Wavenumber (cm^{-1})**		
	pure PVA film	**PVA/OPDC blended film (1.5:0.5 weight ratio)**	**PVA/OPDC blended film (1.0:1.0 weight ratio)**
O-H stretching	3272	3289	3333
C-H stretching	2909	2910	2906
O-H bonding of absorbed water	1658	1652	1648
CH_2 symmetric bonding	1417	1417	1428
C-O-C bending (pyranose ring)	1044	1033	1032
β-glycosidic linkages between glucose	917	918	923

Table 4.5: Summary of ATR spectra of unfilled PVA film and PVA/MCC blended films.

Types of stretching or bending	**Wavenumber (cm^{-1})**		
	pure PVA film	**PVA/MCC blended film (1.5:0.5 weight ratio)**	**PVA/MCC blended film (1.0:1.0 weight ratio)**
O-H stretching	3272	3272	3282
C-H stretching	2909	2910	2913
O-H bonding of absorbed water	1658	1650	1648
CH_2 symmetric bonding	1417	1417	1418
C-O-C bending (pyranose ring)	1044	1041	1033
β-glycosidic linkages between glucose	917	917	918

4.4.2 Tensile Properties

Tensile test was carried out on the PVA/OPDC blended films to determine its tensile strength, elongation at break and elastic modulus in comparison with the properties of PVA/MCC blended films. Figures 4.17 – 4.19 show the tensile strength, elongation at break and elastic modulus of PVA/MCC and PVA/OPDC blended films with different compositions. As shown in Figure 4.17, it can be seen that the tensile strength of PVA/MCC and PVA/OPDC blended films decreased from 35 MPa to 3 MPa and 35 MPa to 9 MPa with increasing MCC and OPDC contents, respectively (Ooi et al., 2011a; Suki, 2014).

The same trend can also be observed for elongation at break in Figure 4.18. It was noticed that pure PVA film has the highest value of elongation at break, which was 377%. However, an addition of 0.5% (wt/wt) MCC and OPDC during the preparation of blended film had adverse effect for elongation at break as a sharp decrease was observed from 377% to 115% and 37%, respectively (Lani et al., 2014; Suki, 2014).

The significant reduction of tensile strength and elongation at break probably indicates the weak intermolecular hydrogen bonding between the cellulose (MCC and OPDC) and PVA. As reported by the researchers, the intramolecular hydrogen bonds cause the OPDC and MCC to agglomerate, which leads to poor dispersion and poor adhesion (Won et al., 2015) of cellulose in the PVA matrix (Ooi et al., 2011a; Suki, Ismail and Hamid, 2014). Besides, the coalesced and coarsely dispersed OPDC granules will act as stress concentrators and will induce the cracks, which then leads to the lower values of tensile strength and elongation at break. According to literature, PVA is hydrophilic while OPDC is semi-hydrophilic due to presence of oils and fats in OPDC, which were not completely removed during pre-treatment. OPDC acted as filler in PVA matrix but as the PVA/OPDC blended films were subjected to the tensile load, only the PVA matrix will mainly withstand the load. This is due to the less effective cross sectional area of OPDC at high OPDC content (Suki, 2014).

The elastic modulus, also known as Young's modulus of PVA/MCC blended film increased from 18 MPa to 125.7 MPa whereas PVA/OPDC blended film increased from 18 MPa to 258 MPa with increasing MCC and OPDC content, respectively as shown in Figure 4.19. This was due to the stiffening effect of MCC and OPDC that restricted the molecular mobility of PVA chain and caused higher resistance of the PVA molecules against straining. Therefore, the presence of MCC and OPDC did not enhance the tensile properties of the blended films due to the poor compatibility of PVA and cellulose (MCC and OPDC) and excellent mechanical properties of PVA itself (Suki, 2014).

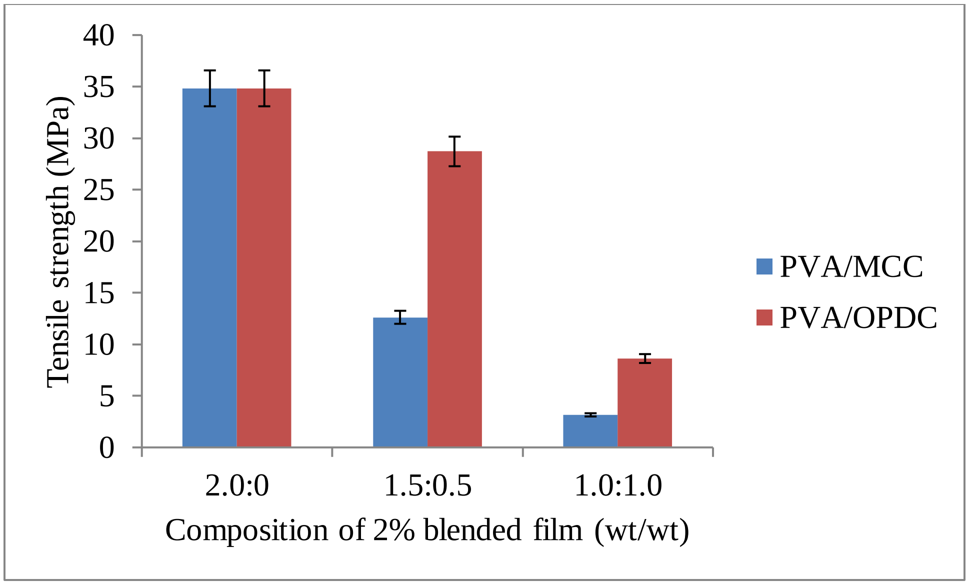

Figure 4.17: Tensile strength of PVA/MCC and PVA/OPDC blended film with different composition.

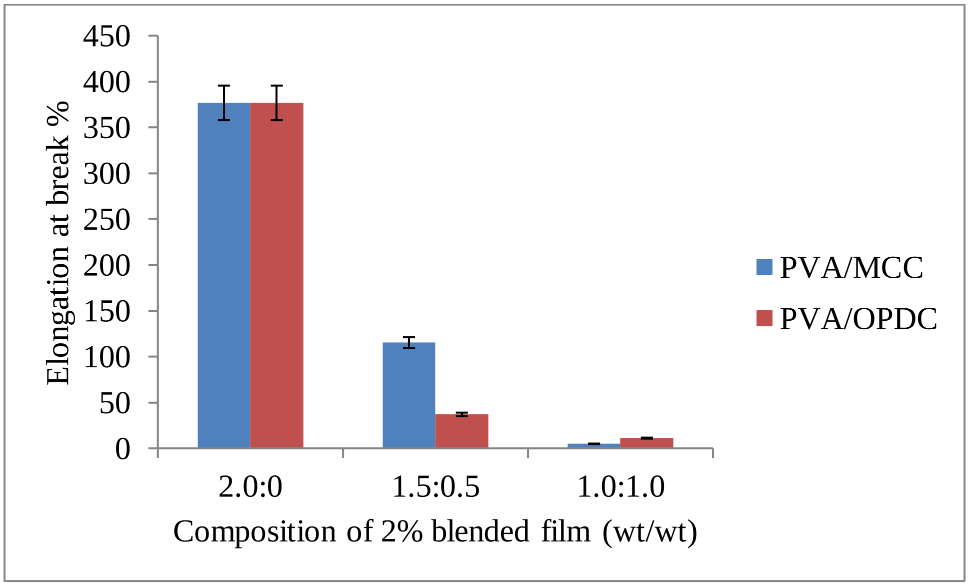

Figure 4.18: Elongation at break of PVA/MCC and PVA/OPDC blended film with different composition.

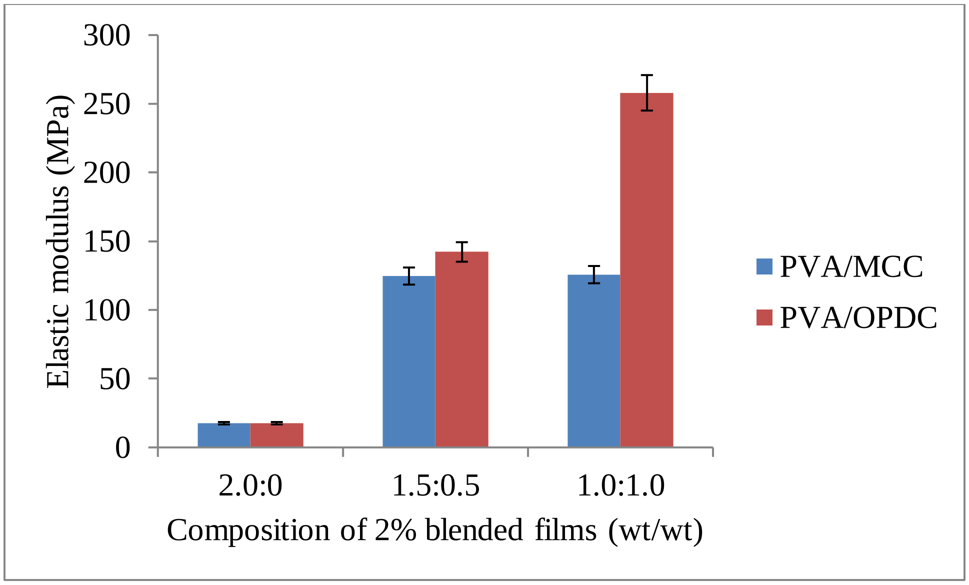

Figure 4.19: Elastic modulus of PVA/MCC and PVA/OPDC blended film with different composition.

In general, PVA/OPDC blended films presented mechanical properties very similar to PVA/MCC blended films, with the advantage of a higher tensile strength and elastic modulus. Thus, the remarkable mechanical properties of PVA/OPDC blended film are promising for biotechnological applications (Fernandes, 2013).

4.4.3 Natural Weathering Test

Figures 4.20 and 4.21 show the percentage of degradation of PVA/OPDC and PVA/MCC blended films with different composition after being exposed to natural weathering for 1 month, respectively. It was found that all the films were highly deteriorated with a decreased value of weight as the week goes. However, all the films have an increase in weight on the third week of exposure due to the effect of rainfall, which caused the films to get moistened and wet whereas water will be removed and dried by strong sunlight. For the unfilled PVA film, the decreased in weight could be attributed to the photooxidation of UV exposure and hydrolysis as a consequence of rainfall and dew. When raining, PVA tends to absorb water due to the presence of hydroxyl groups (Suki, 2014; Sapuan, Ismail and Zainudin, 2018) and therefore resulting in hydrolysis depolymerisation process, which the long polymer chain was converted into smaller oligomer fragments (Bastioli, 2005).

According to Figure 4.20, the percentage of degradation increased with increasing amount of OPDC. The highest weight loss was exhibited by the PVA/OPDC blended film with the ratio 1.0:1.0, which indicates that the loading of OPDC caused the film to degrade easier as compared to the unfilled PVA film and the PVA/OPDC blended film with smaller amount of OPDC. As reported in the literature, cellulose and its derivatives can be easily degraded by microorganisms such as bacteria, fungi and algae present in air, water and soil (Ooi et al., 2011a; Sapuan, Ismail and Zainudin, 2018). The rate of biodegradation of cellulose depends on the cellulose crystallinity. Since OPDC are less crystalline than dissolved pulp, micro/nanoscale cellulose (Zugenmaier, 2008), in this case MCC, PVA/OPDC blended film with greater loading of OPDC has higher biodegradation rate (Khalil et al., 2017).

According to Figure 4.21, it does not show a significant trend of the rate of degradation against the amount of MCC in the film. The highest weight loss was attributed to PVA/MCC blended film with the ratio 1.5:0.5 whereas the lowest weight loss was shown by unfilled PVA film. The results indicate that the biodegradability of PVA/MCC blended film was greatly enhanced when 0.5% wt of MCC was added into the PVA matrix.

Commercial MCC contains a high amount of cellulose by elimination of amorphous cellulose regions and other components such as hemicellulose and lignin during acid hydrolysis (Tan et al., 2015). Due to the highly ordered arrangement of the cellulose, the film will become more compact and thus resistance to penetration of microorganisms into the film for their growth (Chuayjuljit, Su-uthai and Charuchinda, 2010). This explains the reduction in the percentage of degradation as the loading of MCC increased to 1.0% wt. By comparing both of the PVA/MCC blended films with different ratios, the percentage of degradation is lower as the amount of PVA decreased due to lack of water solubility, which prevents microorganisms from carrying the material directly into the film where most biochemical processes take place (Artham and Doble, 2008).

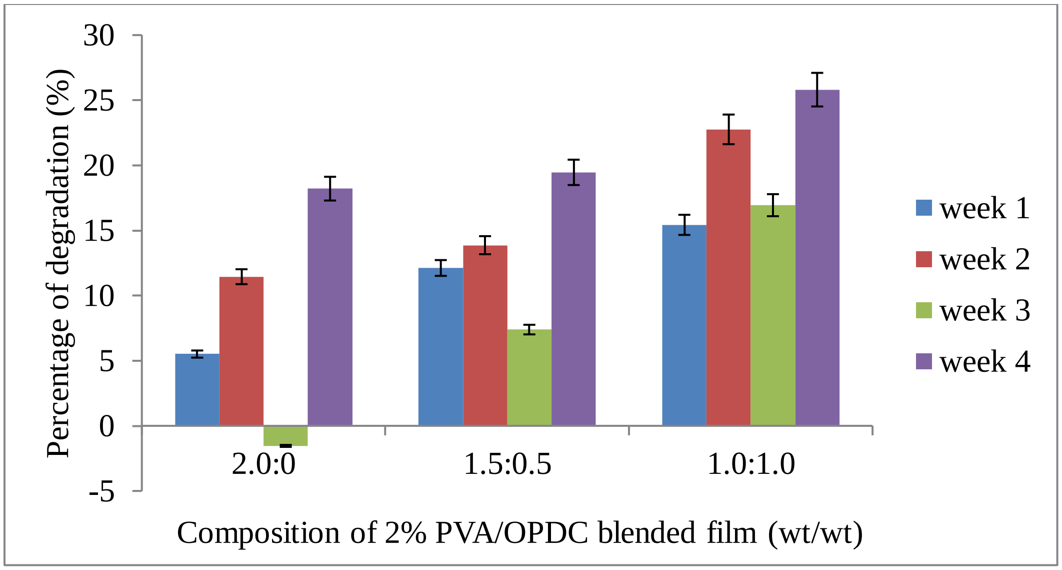

Figure 4.20: The percentage of degradation of PVA/OPDC blended films with different composition after being exposed to natural weathering for 1 month.

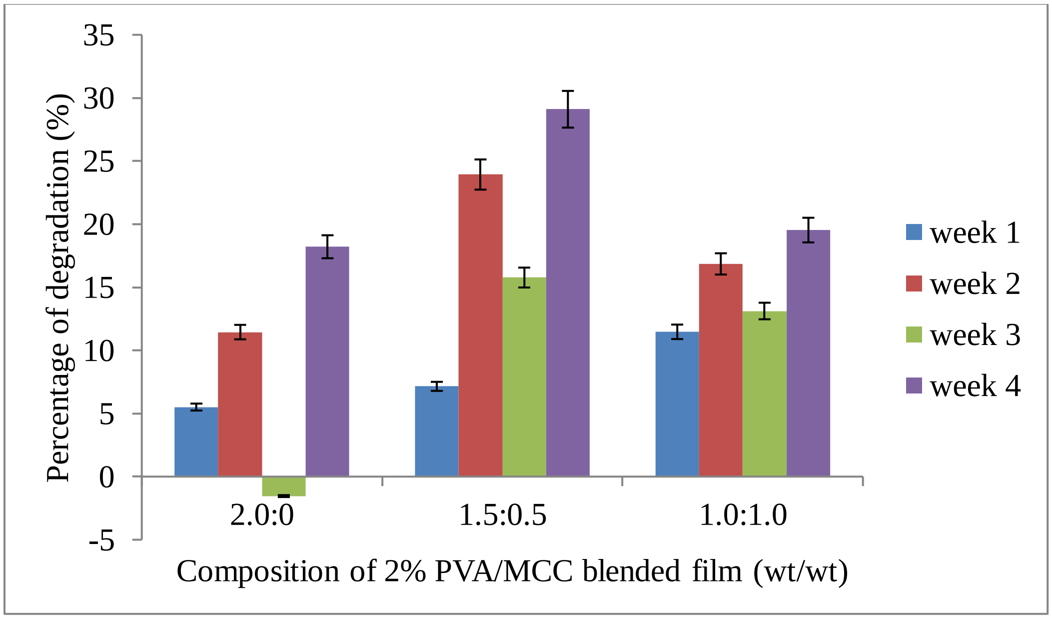

Figure 4.21: The percentage of degradation of PVA/MCC blended films with different composition after being exposed to natural weathering for 1 month.

Figure 4.23 shows the physical appearances of unfilled PVA film whereas Figures 4.24 and 4.25 show the physical appearances of the specimen of PVA/OPDC and PVA/MCC blended film with different composition before and after subjecting to natural weathering, respectively. It is believed that the weathered PVA blended films have experienced substantial changes of stress in the form of swelling and shrinkage, which would cause surface cracking of the films. For instance, the films would absorb water (water absorption) either from humid air or directly get moistened by rain and tend to swell. On the contrary, a subsequent dry period indicates that water is released, which caused shrinkage due to water desorption. The combination of both swelling and shrinkage effect is known as annealing effect, which also contributed to the weight loss of the films. Similar observations were reported by Yew et al. (2009) on PLA/rice starch composites and Ooi et al., (2011a) on PVAOH/JWF films.

One notable observation after 1 week exposure was the adhesion of two unfilled PVA films as shown in Figure 4.23, which were originally hung on the weathering rack separately. PVA is a water-soluble, polar, highly hydrophililc, meaning water absorbing material and biodegradable polymer, which not only possess biocompatibility but also capable of self-cross-linking as shown in Figure 4.22. This is due to the presence of high density of hydroxyl groups situated on its side chains (Miguez-Pacheco, Misra and Boccaccini, 2014).

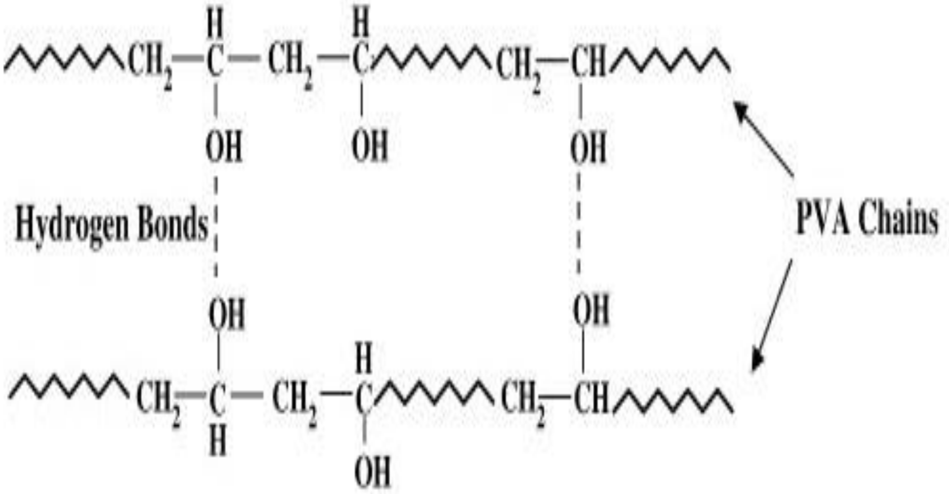

Figure 4.22: The mechanism for cross-linking of pure PVA and hydrogen bonding formation (Bonakdar et al., 2010).

The adhesion of two unfilled PVA films could be due to the effect of strong winds and rainfall. It has been reported that PVA is a self-associated polymer. There is a strong inter- and intramolecular hydrogen bonding formed between the polar hydroxyl groups (– OH - - - OH) in the PVA molecules in addition to the interaction between water molecules and PVA. The extent of both inter- and intramolecular, and PVA-water hydrogen bonding leads to the adhesion of two unfilled PVA films (Briscoe, Luckham and Zhu, 2000; Chen and Zhang, 2010). Also, the unfilled PVA films has bumpy instead of flat surface after exposure for 1 month because of unequal swelling tendencies of the sides of the film (Priest, 1951).

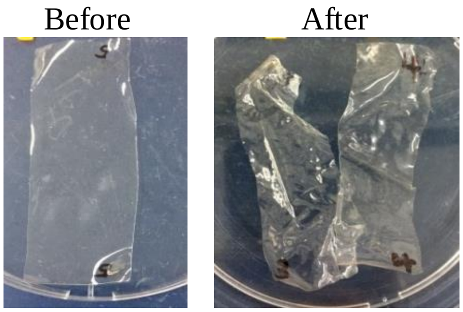

Figure 4.23: Physical appearances of specimen of the unfilled PVA film before and after subjecting to natural weathering.

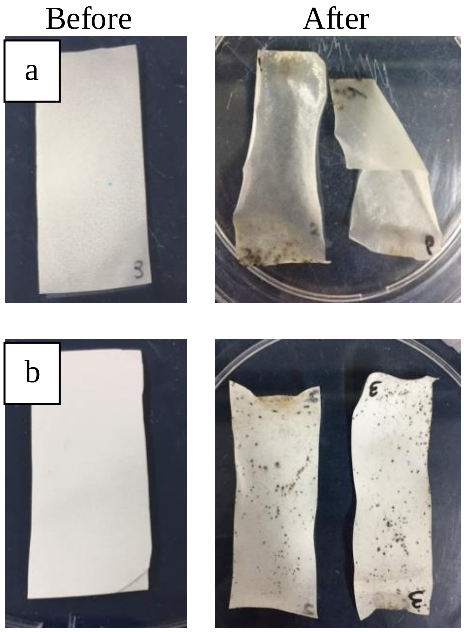

Figure 4.24: Physical appearances of specimens of the PVA/OPDC blended films with weight ratio of (a) 1.5:0.5 and (b) 1.0:1.0 before and after subjecting to natural weathering.

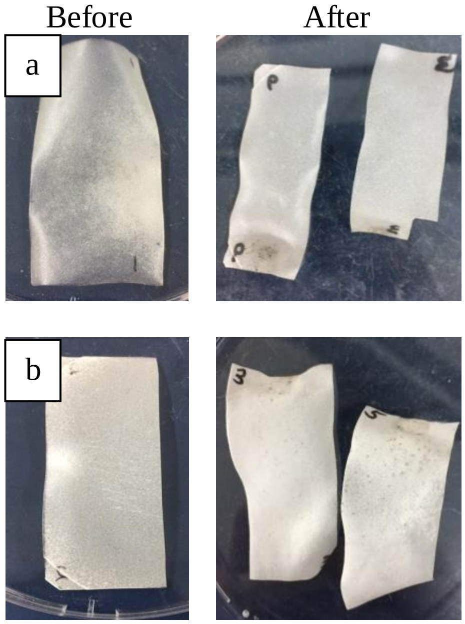

Figure 4.25: Physical appearances of specimens of the PVA/MCC blended films with weight ratio of (a) 1.5:0.5 and (b) 1.0:1.0 before and after subjecting to natural weathering.

It is interestingly noted that tiny black spots have grown on the surface of the film, which reflects the growth of microorganism, which proved that the films are biodegradable. By comparing the PVA/OPDC and PVA/MCC blended films with the ratio of 1.0:1.0, it can be observed that PVA/OPDC blended film has more black spots and thus higher biodegradability. This corresponds to the higher percentage of degradation of PVA/OPDC blended film (26%) in comparison with PVA/MCC blended film (20%).

4.4.4 Morphology Studies of Degraded Films by Field Emission Scanning Electron Microscopy (FESEM)

Figure 4.26 shows the FESEM images of degraded unfilled PVA film after subjected to natural weathering for 1 month with different magnifying power. The cracks on the film as shown in Figure 4.26 (b) indicate that the film has become brittle in nature. The microbial propagation has been initiated from these cracks and consequently the film was being degraded (Shalini and Sasikumar, 2015).

Figures 4.27 and 4.28 show the FESEM images of degraded PVA/MCC and PVA/OPDC blended films after subjected to natural weathering for 1 month with different weight ratios, respectively. It was clearly observed that microbes have grown on the surface of the films, which was indicated by the spherical and rod-like shape microbes. Moreover, the growth of microbes was visible to the naked eye for all the blended films. The pores and rough surface are evident in the FESEM images. As compared to unfilled PVA film, almost whole of the surface of blended films was covered by microbes, which revealed that the growth of microbes was increased when OPDC or MCC was added into the PVA matrix (Suki, 2014). This can be concluded that microbes utilized cellulose and created pores in the PVA film. The morphology studies of degraded films by FESEM have proven the biodegradability of blended by microbes.

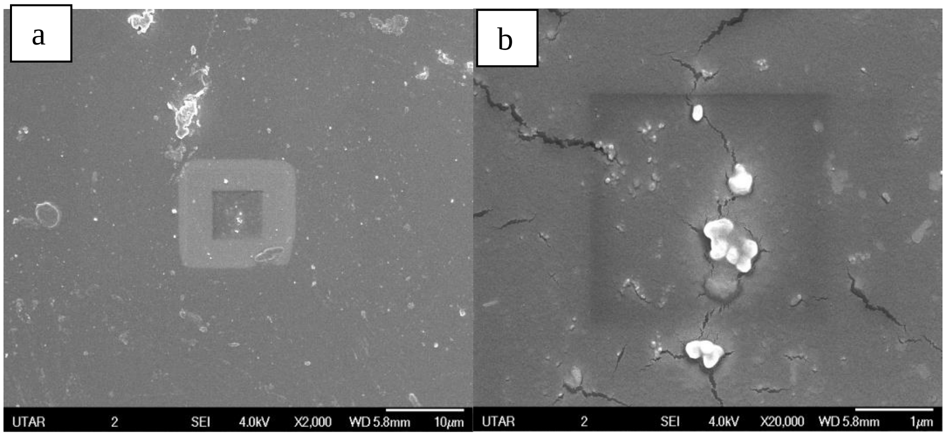

Figure 4.26: FESEM images of degraded unfilled PVA film after subjected to natural weathering for 1 month with the magnifying power of (a) ×2000 and (b) ×20000.

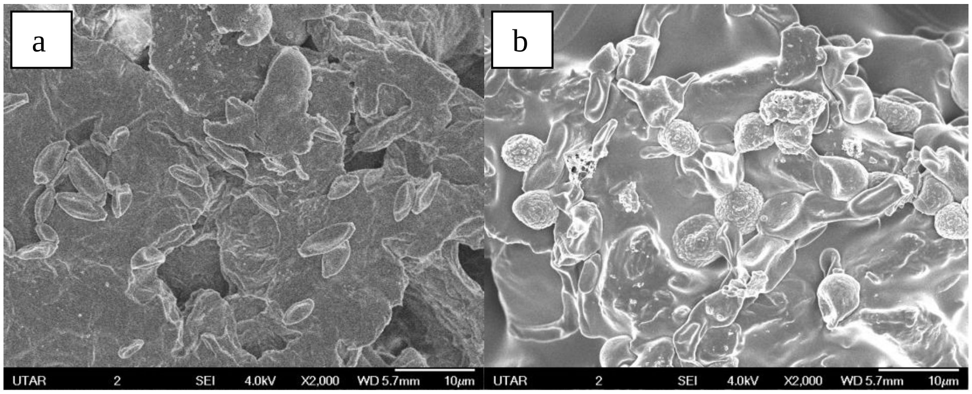

Figure 4.27: FESEM images of degraded PVA/MCC blended films after subjected to natural weathering for 1 month with the composition of (a) 1.5:0.5 and (b) 1.0:1.0.

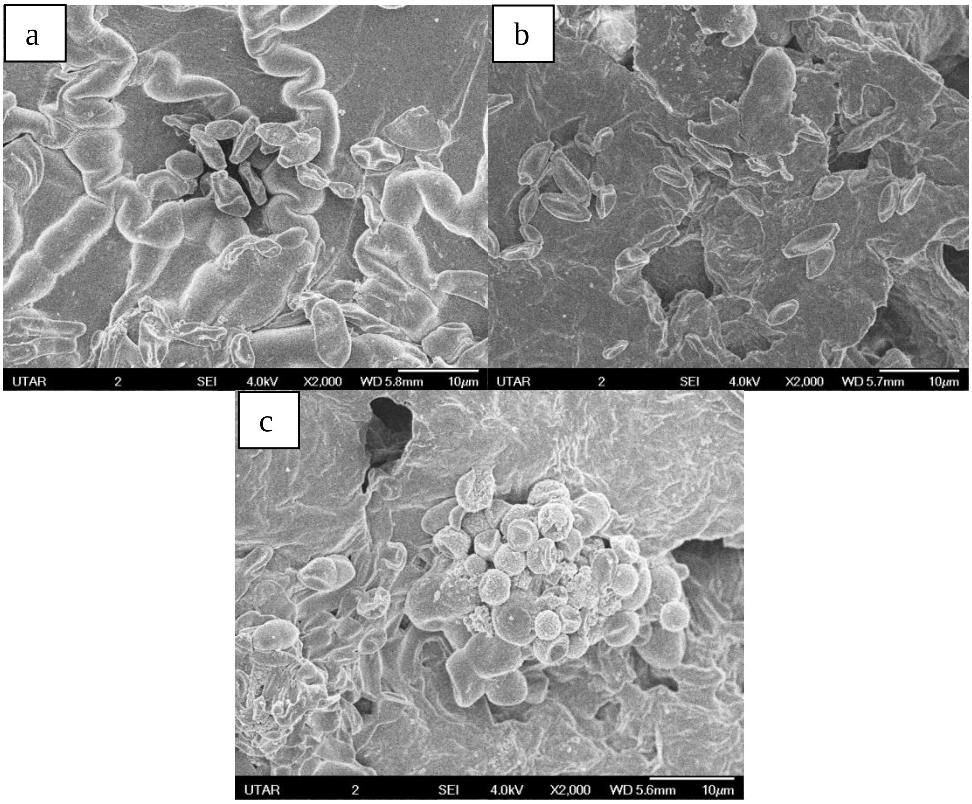

Figure 4.28: FESEM images of degraded PVA/OPDC blended films after subjected to natural weathering for 1 month with the composition of (a) 1.5:0.5, (b) 1.0:1.0 and (c) 0.5:1.5.

CHAPTER 5

CONCLUSIONS

5.1 Conclusions

In this research project, orange peel (OP) was extracted and isolated by alkaline and bleaching treatment to produce cellulose, which was then introduced into the polyvinyl alcohol (PVA) to cast blended films with different weight ratios using solution casting method. The main aim for this research project is to synthesize a biodegradable film with high strength. These environmental friendly degradable films can be applied in many kinds of packaging industries according to their demand in order to reduce the consumption of non-biodegradable materials (plastics) which may lead to environmental problems. In addition, this research project could solve the waste management problem of citrus waste (orange peel). Characterization of the PVA/OPDC blended films was carried out with several analyses to study the effect of OPDC on the properties of film in comparison with PVA/MCC blended films. Based on the results and discussions of this research project, the following conclusions can be made.

I. The cellulose had been extracted and isolated from the OP. It was first subjected to alkaline treatment using sodium hydroxide solution to remove the hemicellulose, and then bleached using acidified sodium chlorite solution to remove lignin. The orange peel derived cellulose (OPDC) was white in colour.

II. The OPDC had been characterized using Attenuated Total Reflectance Spectrometer (ATR), Field Emission Scanning Electron Microscope (FESEM), Particle Size Analyzer, Differential Scanning Calorimetry (DSC) and X-Ray Diffraction (XRD) and compared with MCC. From the ATR spectra, evidence of noncellulosic components removal can be seen, whereby the characteristic peaks of hemicelluloses and lignin around 1736 cm^{-1} and 1236 cm^{-1} had disappeared after treatments. Moreover, the results of FESEM showed the microfibrillated cellulose and particle size analysis revealed that OPDC has become micro-sized after treatments via alkaline and bleaching. According to XRD analysis, the high percentage of crystallinity and sharper diffraction peaks of OPDC after treatments via alkaline and bleaching was due to the removal of hemicellulose and lignin, which exist in the amorphous phase. The appearance of diffraction peaks on the OPDC curve corresponds to the MCC curves, where both of the OPDC and MCC samples possessed a high peak intensity of 2θ angle at 22˚, which was attributed to their crystalline structure of cellulose, whereas the presence of broad peak at around 15˚ indicates the amorphous arrangement. From the DSC analysis, MCC has higher thermal stability than OPDC.

III. The biodegradable blended film with different weight ratio had been prepared from OPDC and MCC with PVA by solution casting method. The transparency of both of the PVA/OPDC and PVA/MCC blended films decreased when the cellulose loading increased due to the decreased homogeneity of the distribution of cellulose in the PVA matrix.

IV. The PVA/OPDC blended film had been characterized and compared with PVA/MCC blended film by Attenuated Total Reflectance Spectrometer (ATR), Field Emission Scanning Electron Microscope (FESEM), tensile test and natural weathering test. According to the ATR spectra, the shift of the characteristic absorption band and the change in intensity of the band observed in the spectra of PVA/OPDC blended films were similar to that of PVA/MCC blended films. This can confirm the development of new inter- and intramolecular hydrogen bonds and a change in the conformation between PVA and cellulose. Based on the tensile test, tensile strength and elongation at break decreased whereas the elastic modulus increased as the amount of cellulose (OPDC and MCC) added was increased. PVA/OPDC blended films presented mechanical properties very similar to PVA/MCC blended films, with the advantage of a higher tensile strength and elastic modulus.Natural weathering test revealed that unfilled PVA, PVA/OPDC and PVA/MCC blended films had experienced weight with longer period of exposure.The highest weight loss was exhibited by the PVA/OPDC blended film with the ratio 1.0:1.0, which indicates that the loading of OPDC caused the film to degrade easier as compared to the unfilled PVA film and the PVA/OPDC blended film with smaller amount of OPDC. On the contrary, PVA/MCC blended film with the ratio 1.5:0.5 exhibited the highest weight loss, which indicates that the biodegradability of PVA/MCC blended film was greatly enhanced when 0.5% wt of MCC was added into the PVA matrix. Tiny black spots on the surface of the film reflect the growth of microorganism, which proved that the films are biodegradable. By comparing the PVA/OPDC and PVA/MCC blended films with the ratio of 1.0:1.0, it can be observed that PVA/OPDC blended film has more black spots and thus higher biodegradability. This corresponds to the higher percentage of degradation of PVA/OPDC blended film in comparison with PVA/MCC blended film. The growth of microorganisms was further proven by the surface morphologies of degraded films by FESEM.

5.2 Recommendations for Future Work

Based on the results and discussions of this research project, there are more to be investigated in order to improve the results in further studies. Below are some recommendations for the future works:

I. The whole process of the extraction and isolation of cellulose is time-consuming. Other methods and reaction conditions for the extraction and isolation of cellulose can be employed to reduce the duration of the whole process as well as improve the yield of cellulose.

II. Acid hydrolysis study should be considered to improve the size of cellulose in the nano range in order to further enhance the properties of orange peel filled polyvinyl alcohol blends.

III. Further studies on the properties of the PVA/OPDC blended film can be conducted such as the water absorption test, soil burial degradation test and thermal characterization.

IV. Further studies on suitable crosslinking agents, plasticizers and other additives are needed to improved mechanical properties of the PVA/OPDC blended films.

V. Further analysis on the natural weathering degraded films could be considered to determine the types of microorganisms which grow on the surface of degraded films.

REFERENCES

Abdel-Halim, E.S., 2013. Amine salts-activated systems for one-step bleaching of cotton fabrics. *Carbohydrate polymers*, *96*(1), pp.64-70.

Abdel-Halim, E.S., 2014. Chemical modification of cellulose extracted from sugarcane bagasse: Preparation of hydroxyethyl cellulose. *Arabian Journal of Chemistry*, *7*(3), pp.362-371.

Abraham, E., Deepa, B., Pothan, L.A., Jacob, M., Thomas, S., Cvelbar, U. and Anandjiwala, R., 2011. Extraction of nanocellulose fibrils from lignocellulosic fibres: A novel approach. *Carbohydrate Polymers*, *86*(4), pp.1468-1475.

Adamcová, D. and Vaverková, M., 2014. Degradation of Biodegradable/Degradable Plastics in Municipal Solid-Waste Landfill. *Polish Journal of Environmental Studies*, *23*(4).

Artham, T. and Doble, M., 2008. Biodegradation of aliphatic and aromatic polycarbonates. *Macromolecular bioscience*, *8*(1), pp.14-24.

Attia, G. and El-Kader, M.A., 2013. Structural, optical and thermal characterization of PVA/2HEC polyblend films. *Int. J. Electrochem. Sci*, *8*, pp.5672-5687.

Balu, A.M., Budarin, V., Shuttleworth, P.S., Pfaltzgraff, L.A., Waldron, K., Luque, R. and Clark, J.H., 2012. Valorisation of orange peel residues: waste to biochemicals and nanoporous materials. *ChemSusChem*, *5*(9), pp.1694-1697.

Bastioli, C. ed., 2005. *Handbook of biodegradable polymers*. iSmithers Rapra Publishing.

Bátori, V., Jabbari, M., Åkesson, D., Lennartsson, P.R., Taherzadeh, M.J. and Zamani, A., 2017. Production of pectin-cellulose biofilms: A new approach for citrus waste recycling. *International Journal of Polymer Science*, *2017*.

Béguin, P. and Aubert, J.P., 1994. The biological degradation of cellulose. *FEMS microbiology reviews*, *13*(1), pp.25-58.

Berglund, L., Noël, M., Aitomäki, Y., Öman, T. and Oksman, K., 2016. Production potential of cellulose nanofibers from industrial residues: Efficiency and nanofiber characteristics. *Industrial Crops and Products*, *92*, pp.84-92.

Bicu, I. and Mustata, F., 2011. Cellulose extraction from orange peel using sulfite digestion reagents. *Bioresource technology*, *102*(21), pp.10013-10019.

Bonakdar, S., Emami, S.H., Shokrgozar, M.A., Farhadi, A., Ahmadi, S.A.H. and Amanzadeh, A., 2010. Preparation and characterization of polyvinyl alcohol hydrogels crosslinked by biodegradable polyurethane for tissue engineering of cartilage. *Materials science and engineering: c*, *30*(4), pp.636-643.

Briscoe, B., Luckham, P. and Zhu, S., 2000. The effects of hydrogen bonding upon the viscosity of aqueous poly (vinyl alcohol) solutions. *Polymer*, *41*(10), pp.3851-3860.

Carr, D.P., 2012. *Assessment of alternative uses for lignocellulosic waste products* (Doctoral dissertation, National University of Ireland Maynooth).

Chen, H., 2014. Chemical composition and structure of natural lignocellulose. In *Biotechnology of lignocellulose* (pp. 25-71). Springer, Dordrecht.

Chen, H., Yu, Y., Zhong, T., Wu, Y., Li, Y., Wu, Z. and Fei, B., 2017. Effect of alkali treatment on microstructure and mechanical properties of individual bamboo fibers. *Cellulose*, *24*(1), pp.333-347.

Chen, N.X. and Zhang, J.H., 2010. The role of hydrogen-bonding interaction in poly (vinyl alcohol)/poly (acrylic acid) blending solutions and their films. *Chinese Journal of Polymer Science*, *28*(6), pp.903-911.

Chen, X., Wu, S., Yi, M., Ge, J., Yin, G. and Li, X., 2018. Preparation and physicochemical properties of blend films of feather keratin and poly (vinyl alcohol) compatibilized by tris (hydroxymethyl) aminomethane. *Polymers*, *10*(10), p.1054.

Chen, Y., Cao, X., Chang, P.R. and Huneault, M.A., 2008. Comparative study on the films of poly (vinyl alcohol)/pea starch nanocrystals and poly (vinyl alcohol)/native pea starch. *Carbohydrate Polymers*, *73*(1), pp.8-17.

Choi, M., Kang, Y.R., Lim, I.S. and Chang, Y.H., 2018. Structural Characterization of Cellulose Obtained from Extraction Wastes of Graviola (Annona muricata) Leaf. *Preventive nutrition and food science*, *23*(2), p.166.

Choo, K., Ching, Y., Chuah, C., Julai, S. and Liou, N.S., 2016. Preparation and characterization of polyvinyl alcohol-chitosan composite films reinforced with cellulose nanofiber. *Materials*, *9*(8), p.644.

Choudhury, A.R., 2011. Pre-treatment and preparation of textile materials prior to dyeing. In *Handbook of Textile and Industrial Dyeing* (pp. 64-149).

Chieng, B., Lee, S., Ibrahim, N., Then, Y. and Loo, Y., 2017. Isolation and characterization of cellulose nanocrystals from oil palm mesocarp fiber. *Polymers*, *9*(8), p.355.

Ching, Y.C., Rahman, A., Ching, K.Y., Sukiman, N.L. and Cheng, H.C., 2015. Preparation and characterization of polyvinyl alcohol-based composite reinforced with nanocellulose and nanosilica. *BioResources*, *10*(2), pp.3364-3377.

Chuayjuljit, S., Su-uthai, S. and Charuchinda, S., 2010. Poly (vinyl chloride) film filled with microcrystalline cellulose prepared from cotton fabric waste: properties and biodegradability study. Waste Management and Research, 28(2), pp.109-117.

Ciolacu, D., Ciolacu, F. and Popa, V.I., 2011. Amorphous cellulose—structure and characterization. *Cellulose chemistry and technology*, *45*(1), p.13.

Deng, G.F., Shen, C., Xu, X.R., Kuang, R.D., Guo, Y.J., Zeng, L.S., Gao, L.L., Lin, X., Xie, J.F., Xia, E.Q. and Li, S., 2012. Potential of fruit wastes as natural resources of bioactive compounds. *International journal of molecular sciences*, *13*(7), pp.8308-8323.

Egüés, I., Sanchez, C., Mondragon, I. and Labidi, J., 2012. Effect of alkaline and autohydrolysis processes on the purity of obtained hemicelluloses from corn stalks. *Bioresource technology*, *103*(1), pp.239-248.

Eich, A., Mildenberger, T., Laforsch, C. and Weber, M., 2015. Biofilm and diatom succession on polyethylene (PE) and biodegradable plastic bags in two marine habitats: early signs of degradation in the pelagic and benthic zone?. *PLoS One*, *10*(9), p.e0137201.

Fan, M., Dai, D. and Huang, B., 2012. Fourier transform infrared spectroscopy for natural fibres. In *Fourier transform-materials analysis*. Intechopen.

Fernandes, K.F., 2013. PVA/polysaccharides blended films: mechanical properties. *Journal of Materials*, *2013*.

Frone, A.N., Nicolae, C.A., Gabor, R.A. and Panaitescu, D.M., 2015. Thermal properties of water-resistant starch–polyvinyl alcohol films modified with cellulose nanofibers. *Polymer degradation and stability*, *121*, pp.385-397.

Gandini, A. and Belgacem, M.N., 2013. The state of the art of polymers from renewable resources. In *Handbook of Biopolymers and Biodegradable Plastics* (pp. 71-85).

Grönqvist, S., Hakala, T.K., Kamppuri, T., Vehviläinen, M., Hänninen, T., Liitiä, T., Maloney, T. and Suurnäkki, A., 2014. Fibre porosity development of dissolving pulp during mechanical and enzymatic processing. *Cellulose*, *21*(5), pp.3667-3676.

Hariani, P.L., Riyanti, F. and Asmara, R.D., 2016. Extraction of Cellulose from Kepok Banana Peel (Musa parasidiaca L.) for Adsorption Procion Dye. *Molekul*, *11*(1), pp.135-142.

Hospodarova, V., Singovszka, E. and Stevulova, N., 2018. Characterization of Cellulosic Fibers by FTIR Spectroscopy for Their Further Implementation to Building Materials. *American Journal of Analytical Chemistry*, *9*(06), p.303.

Hussin, M.H., Husin, N.A., Bello, I., Othman, N., Bakar, M.A. and Haafiz, M.M., 2018. Isolation of Microcrystalline Cellulose (MCC) from Oil Palm Frond as Potential Natural Filler for PVA-LiClO4 Polymer Electrolyte. *Int. J. Electrochem. Sci*, *13*, pp.3356-3371.

Ibrahim, M.M., El-Zawawy, W.K. and Nassar, M.A., 2010. Synthesis and characterization of polyvinyl alcohol/nanospherical cellulose particle films. *Carbohydrate polymers*, *79*(3), pp.694-699.

Ilyas, R.A., Sapuan, S.M. and Ishak, M.R., 2018. Isolation and characterization of nanocrystalline cellulose from sugar palm fibres (ArengaPinnata). *Carbohydrate polymers*, *181*, pp.1038-1051.

Ishigaki, T., Kawagoshi, Y., Ike, M. and Fujita, M., 1999. Biodegradation of a polyvinyl alcohol-starch blend plastic film. *World Journal of Microbiology and Biotechnology*, *15*(3), pp.321-327.

Jeffries, T.W., 1994. Biodegradation of lignin and hemicelluloses. In *Biochemistry of microbial degradation* (pp. 233-277). Springer, Dordrecht.

John, M.J. and Thomas, S., 2008. Biofibres and biocomposites. *Carbohydrate polymers*, *71*(3), pp.343-364.

Jung, S.J., Kim, S.H. and Chung, I.M., 2015. Comparison of lignin, cellulose, and hemicellulose contents for biofuels utilization among 4 types of lignocellulosic crops. *Biomass and Bioenergy*, *83*, pp.322-327.

Khalil, H.P.S., Tye, Y.Y., Saurabh, C.K., Leh, C.P., Lai, T.K., Chong, E.W.N., Fazita, M.R., Hafiidz, J.M., Banerjee, A. and Syakir, M.I., 2017. Biodegradable polymer films from seaweed polysaccharides: A review on cellulose as a reinforcement material. *Express Polymer Letters*, *11*(4).

Kord, B., Malekian, B., Yousefi, H. and Najafi, A., 2016. Preparation and characterization of nanofibrillated Cellulose/Poly (Vinyl Alcohol) composite films. *Maderas. Ciencia y tecnología*, *18*(4), pp.743-752.

Kumar, A., Negi, Y.S., Choudhary, V. and Bhardwaj, N.K., 2014. Characterization of cellulose nanocrystals produced by acid-hydrolysis from sugarcane bagasse as agro-waste. *Journal of Materials Physics and Chemistry*, *2*(1), pp.1-8.

Kuthi, F.A.A., Norzali, N.R.A.A. and Badri, K.H., 2016. Thermal characteristics of microcrystalline cellulose from oil palm biomass. *Malaysian Journal of Analytical Sciences*, *20*(5), pp.1112-1122.

Lani, N.S., Ngadi, N., Johari, A. and Jusoh, M., 2014. Isolation, characterization, and application of nanocellulose from oil palm empty fruit bunch fiber as nanocomposites. *Journal of Nanomaterials, 2014,* p.13.

Lavanya, D., Kulkarni, P.K., Dixit, M., Raavi, P. and Krishna, L., 2011. Sources of cellulose and their applications—a review. *Int J Drug Formul Res*, *2,* p.2.

Li, J., Liu, Y., Duan, C., Zhang, H. and Ni, Y., 2015. Mechanical pretreatment improving hemicelluloses removal from cellulosic fibers during cold caustic extraction. *Bioresource technology*, *192*, pp.501-506.

Liang, S., Huang, Q., Liu, L. and Yam, K.L., 2009. Microstructure and molecular interaction in glycerol plasticized chitosan/poly (vinyl alcohol) blending films. *Macromolecular chemistry and physics*, *210*(10), pp.832-839.

Liew, F.K., Hamdan, S., Rahman, M., Rusop, M., Lai, J.C.H. and Hossen, M., 2015. Synthesis and characterization of cellulose from green bamboo by chemical treatment with mechanical process. *Journal of Chemistry*, *2015*.

Liu, H., You, L., Jin, H. and Yu, W., 2013. Influence of alkali treatment on the structure and properties of hemp fibers. *Fibers and polymers*, *14*(3), pp.389-395.

Liu, W., Mohanty, A.K., Drzal, L.T., Askel, P. and Misra, M., 2004. Effects of alkali treatment on the structure, morphology and thermal properties of native grass fibers as reinforcements for polymer matrix composites. *Journal of Materials Science*, *39*(3), pp.1051-1054.

López, J.A.S., Li, Q. and Thompson, I.P., 2010. Biorefinery of waste orange peel. *Critical Reviews in Biotechnology*, *30*(1), pp.63-69.

Lu, J., Wang, T. and Drzal, L.T., 2008. Preparation and properties of microfibrillated cellulose polyvinyl alcohol composite materials. *Composites Part A: Applied Science and Manufacturing*, *39*(5), pp.738-746.

Lu, P. and Hsieh, Y.L., 2010. Preparation and properties of cellulose nanocrystals: rods, spheres, and network. *Carbohydrate polymers*, *82*(2), pp.329-336.

Luo, X. and Wang, X., 2017. Preparation and characterization of nanocellulose fibers from NaOH/Urea pretreatment of oil palm fibers. *BioResources*, *12*(3), pp.5826-5837.

Mali, S., Sakanaka, L.S., Yamashita, F. and Grossmann, M.V.E., 2005. Water sorption and mechanical properties of cassava starch films and their relation to plasticizing effect. *Carbohydrate Polymers, 60*(3), pp.283-289.

Malini, R., Tajuddin, R.M. and Hamid, N. S. A., 2018. Citrus fruit waste leachate treatment by using newly developed flat sheet membrane. *International Journal of Scientific and Research Publications*, 8(3), pp.83-89.

Mamma, D., Kourtoglou, E. and Christakopoulos, P., 2008. Fungal multienzyme production on industrial by-products of the citrus-processing industry. *Bioresource technology*, *99*(7), pp.2373-2383.

Miguez-Pacheco, V., Misra, S.K. and Boccaccini, A.R., 2014. Biodegradable and bioactive polymer/inorganic phase nanocomposites for bone tissue engineering (BTE). In *Tissue Engineering Using Ceramics and Polymers* (pp. 115-150). Woodhead Publishing.

Moon, R.J., Martini, A., Nairn, J., Simonsen, J. and Youngblood, J., 2011. Cellulose nanomaterials review: structure, properties and nanocomposites. *Chemical Society Reviews, 40*(7), pp.3941-3994.

Mussatto, S.I., Rocha, G.J. and Roberto, I.C., 2008. Hydrogen peroxide bleaching of cellulose pulps obtained from brewer’s spent grain. *Cellulose*, *15*(4), pp.641-649.

Mzimela, Z.N.T., Linganiso, L.Z., Revaprasadu, N. and Motaung, T.E., 2018. Comparison of Cellulose Extraction from Sugarcane Bagasse Through Alkali. *Materials Research*, *21*(6).

Naduparambath, S., Sreejith, M.P., Jinitha, T.V., Shaniba, V., Aparna, K.B. and Purushothaman, E., 2018. Development of green composites of poly (vinyl alcohol) reinforced with microcrystalline cellulose derived from sago seed shells. *Polymer Composites*, *39*(9), pp.3033-3039.

Naz, S., Ahmad, N., Akhtar, J., Ahmad, N.M., Ali, A. and Zia, M., 2016. Management of citrus waste by switching in the production of nanocellulose. *IET nanobiotechnology*, *10*(6), pp.395-399.

O’Brine, T. and Thompson, R.C., 2010. Degradation of plastic carrier bags in the marine environment. *Marine pollution bulletin*, *60*(12), pp.2279-2283.

Oksman, K., Mathew, A.P., Bismarck, A., Rojas, O. and Sain, M., 2014. Handbook of Green Materials: Processing Technologies, Properties and Applications. [e-book] Singapore: World Scientific Publishing Co. Pte. Ltd. Available at: Goggle Bookshttps://books.google.com.my/books?id=gunTelbEtuMC&printsec=frontcover&#v=snippet&q=solution%20casting%20&f=false [Accessed 24 January 2019].

Ooi, Z.X., Ismail, H., Bakar, A.A. and Aziz, N.A.A., 2011a. Effects of jackfruit waste flour on the properties of poly (vinyl alcohol) film. *Journal of Vinyl and Additive Technology*, *17*(3), pp.198-208.

Ooi, Z.X., Ismail, H., Bakar, A.A. and Aziz, N.A.A., 2011b. Preparation and properties of biodegradable polymer film based on polyvinyl alcohol and tropical fruit waste flour. *Polymer-Plastics Technology and Engineering*, *50*(7), pp.705-711.

Ooi, Z.X., Ismail, H., Bakar, A.A. and Aziz, N.A.A., 2012a. Properties of the crosslinked plasticized biodegradable poly (vinyl alcohol)/rambutan skin waste flour blends. *Journal of Applied Polymer Science*, *125*(2), pp.1127-1135.

Ooi, Z.X., Ismail, H., Bakar, A.A. and Aziz, N.A.A., 2012b. The comparison effect of sorbitol and glycerol as plasticizing agents on the properties of biodegradable polyvinyl alcohol/rambutan skin waste flour blends. *Polymer-Plastics Technology and Engineering*, *51*(4), pp.432-437.

Othman, N., Azahari, N.A. and Ismail, H., 2011. Thermal properties of polyvinyl alcohol (PVOH)/corn starch blend film. *Malaysin Polymer Journal*, 6(6), pp.147-154.

Pelissari, F.M., do Amaral Sobral, P.J. and Menegalli, F.C., 2014. Isolation and characterization of cellulose nanofibers from banana peels. *Cellulose*, *21*(1), pp.417-432.

Pérez, J., Munoz-Dorado, J., de la Rubia, T.D.L.R. and Martinez, J., 2002. Biodegradation and biological treatments of cellulose, hemicellulose and lignin: an overview. *International microbiology*, *5*(2), pp.53-63.

Price, A. J. and Kelton, J., 2013. Herbicides. 1st ed. Rijeka, Croatia: Intech, pp.1-320.

Priest, W.J., 1951. Swelling of polyvinyl alcohol in water. *Journal of Polymer Science*, *6*(6), pp.699-710.

Prieto, A., 2016. To be, or not to be biodegradable… that is the question for the bio-based plastics. *Microbial biotechnology*, *9*(5), pp.652-657.

Qdais, H.A., Abdulla, F. and Qrenawi, L., 2010. Solid waste landfills as a source of green energy: Case study of Al Akeeder landfill. *JJMIE*, *4*(1).

Rahman, M.M., Afrin, S. and Haque, P., 2014. Characterization of crystalline cellulose of jute reinforced poly (vinyl alcohol) (PVA) biocomposite film for potential biomedical applications. *Progress in biomaterials*, *3*(1), p.23.

Rahman, W.A., Ismail, S.N.A.S. and Rosli, M., 2016, October. Morphology and properties of durian cellulose nanofibres reinforced polyvinyl alcohol/starch based composite. In *AIP Conference Proceedings* (Vol. 1774, No. 1, p. 020005). AIP Publishing.

Ramaraj, B., 2006. Modified poly (vinyl alcohol) and coconut shell powder composite films: Physico-mechanical, thermal properties, and swelling studies. *Polymer-Plastics Technology and Engineering*, *45*(11), pp.1227-1231.

Reddy, N. and Yang, Y., 2009. Extraction and characterization of natural cellulose fibers from common milkweed stems. *Polymer Engineering & Science*, *49*(11), pp.2212-2217.

Renou, S., Givaudan, J.G., Poulain, S., Dirassouyan, F. and Moulin, P., 2008. Landfill leachate treatment: review and opportunity. *Journal of hazardous materials*, *150*(3), pp.468-493.

Riley, A., 2012. Plastics manufacturing processes for packaging materials. In *Packaging Technology* (pp. 310-360).

Roohani, M., Habibi, Y., Belgacem, N.M., Ebrahim, G., Karimi, A.N. and Dufresne, A., 2008. Cellulose whiskers reinforced polyvinyl alcohol copolymers nanocomposites. *European polymer journal*, *44*(8), pp.2489-2498.

Roussos, P.A., 2011. Phytochemicals and antioxidant capacity of orange (Citrus sinensis (l.) Osbeck cv. Salustiana) juice produced under organic and integrated farming system in Greece. *Scientia horticulturae*, *129*(2), pp.253-258.

Rowell, R.M., 1992. *Opportunities for lignocellulosic materials and composites* (pp. 12-27). American Chemical Society.

Saha, P., Manna, S., Chowdhury, S.R., Sen, R., Roy, D. and Adhikari, B., 2010. Enhancement of tensile strength of lignocellulosic jute fibers by alkali-steam treatment. *Bioresource technology*, *101*(9), pp.3182-3187.

Sapuan, S.M., Ismail, H. and Zainudin, E.S., 2018. *Natural Fiber Reinforced Vinyl Ester and Vinyl Polymer Composites: Development, Characterization and Applications*. Woodhead Publishing.

Sarwar, M.S., Niazi, M.B.K., Jahan, Z., Ahmad, T. and Hussain, A., 2018. Preparation and characterization of PVA/nanocellulose/Ag nanocomposite films for antimicrobial food packaging. *Carbohydrate polymers*, *184*, pp.453-464.

Scheirs, J., 2000. *Compositional and failure analysis of polymers: a practical approach*. John Wiley & Sons.

Sgriccia, N., Hawley, M.C. and Misra, M., 2008. Characterization of natural fiber surfaces and natural fiber composites. *Composites Part A: Applied Science and Manufacturing*, *39*(10), pp.1632-1637.

Shalini, R and Sasikumar, C., 2015. Effect of microbes on low density polyethylene material degradation with reference to SEM analysis. *International Journal of Pharma and Bio Sciences*, *6(4)*, pp.447-452.

Siddaiah, T., Ojha, P., Kumar, N.O. and Ramu, C., 2018. Structural, optical and thermal characterizations of PVA/MAA: EA polyblend films. *Materials Research*, *21*(5).

Sreekumar, P.A., Manirul Haque, S.K., Afzal, H.M., Sadique, Z. and Al-Harthi, M.A., 2018. Preparation and characterization of microcellulose reinforced polyvinyl alcohol/starch biocomposites. *Journal of Composite Materials*, p.0021998318816437.

Sudhamani, S.R., Prasad, M.S. and Sankar, K.U., 2003. DSC and FTIR studies on gellan and polyvinyl alcohol (PVA) blend films. *Food Hydrocolloids*, *17*(3), pp.245-250.

Suki, F.M.M., 2014. *Preparation and Properties of Polyvinyl Alcohol/soya Bean Flour Biodegradable Film* (Doctoral dissertation, Universiti Sains Malaysia).

Suki, F.M.M., Ismail, H. and Hamid, Z.A.A., 2013. Effect of Soya Bean Flour Content on Mechanical Properties and Biodegradability of Poly (vinyl alcohol) Film. In *Advanced Materials Research* (Vol. 626, pp. 360-365). Trans Tech Publications.

Suki, F.M.M., Ismail, H. and Hamid, Z.A.A., 2014. Preparation and Properties of Polyvinyl Alcohol/Banana Frond Flour Biodegradable Film. *Progress in Rubber, Plastics and Recycling Technology*, *30*(2), p.103.

Szymańska-Chargot, M., Chylińska, M., Gdula, K., Kozioł, A. and Zdunek, A., 2017. Isolation and characterization of cellulose from different fruit and vegetable pomaces. *Polymers*, *9*(10), p.495.

Taib, R.M., Ghaleb, Z.A. and Mohd Ishak, Z.A., 2012. Thermal, mechanical, and morphological properties of polylactic acid toughened with an impact modifier. *Journal of applied polymer science*, *123*(5), pp.2715-2725.

Tan, B.K., Ching, Y.C., Poh, S.C., Abdullah, L.C. and Gan, S.N., 2015. A review of natural fiber reinforced poly (vinyl alcohol) based composites: Application and opportunity. *Polymers*, *7*(11), pp.2205-2222.

Tang, S., Zou, P., Xiong, H. and Tang, H., 2008. Effect of nano-SiO2 on the performance of starch/polyvinyl alcohol blend films. *Carbohydrate polymers*, *72*(3), pp.521-526.

Taylor, R.F. and Schultz, J.S., 1996. Handbook of Chemical and Biological Sensors. [e-book] London: Institute of Physics Publishing. Available at: Goggle Books https://books.google.com.my/books?id=gunTelbEtuMC&printsec=frontcover&#v=snippet&q=solution%20casting%20&f=false [Accessed 24 January 2019].

Trache, D., Donnot, A., Khimeche, K., Benelmir, R. and Brosse, N., 2014. Physico-chemical properties and thermal stability of microcrystalline cellulose isolated from Alfa fibres. *Carbohydrate polymers*, *104*, pp.223-230.

Wan, J., Wang, Y. and Xiao, Q., 2010. Effects of hemicellulose removal on cellulose fiber structure and recycling characteristics of eucalyptus pulp. *Bioresource technology*, *101*(12), pp.4577-4583.

Wang, J., Li, Y., Wang, Z., Li, Y. and Liu, N., 2016. Influence of pretreatment on properties of cotton fiber in aqueous NaOH/urea solution. *Cellulose*, *23*(3), pp.2173-2183.

Wang, Y.C., Chuang, Y.C. and Hsu, H.W., 2008. The flavonoid, carotenoid and pectin content in peels of citrus cultivated in Taiwan. *Food chemistry*, *106*(1), pp.277-284.

Wei, L., Yan, T., Wu, Y., Chen, H. and Zhang, B., 2018. Optimization of alkaline extraction of hemicellulose from sweet sorghum bagasse and its direct application for the production of acidic xylooligosaccharides by Bacillus subtilis strain MR44. *PloS one*, *13*(4), p.e 0195616.

Won, J.S., Lee, J.E., Jin, D.Y. and Lee, S.G., 2015. Mechanical properties and biodegradability of the kenaf/soy protein isolate-PVA biocomposites. *International Journal of Polymer Science*, *2015*.

Yang, H., Yan, R., Chen, H., Lee, D.H. and Zheng, C., 2007. Characteristics of hemicellulose, cellulose and lignin pyrolysis. *Fuel*, *86*(12-13), pp.1781-1788.

Yew, G.H., Chow, W.S., Mohd Ishak, Z.A. and Mohd Yusof, A.M., 2009. Natural weathering of poly (lactic acid): effects of rice starch and epoxidized natural rubber. *Journal of Elastomers & Plastics*, *41*(4), pp.369-382.

Zain, N.F.M., Yusop, S.M. and Ahmad, I., 2014. Preparation and characterization of cellulose and nanocellulose from pomelo (Citrus grandis) albedo. *J Nutr Food Sci*, *5*(1), pp.1-4

Zarina, S. and Ahmad, I., 2014. Biodegradable composite films based on κ-carrageenan reinforced by cellulose nanocrystal from kenaf fibers. *BioResources*, *10*(1), pp.256-271.

Zhang, L., Liu, H., Zheng, L., Zhang, J., Du, Y. and Feng, H., 1996. Biodegradability of regenerated cellulose films in soil. *Industrial & engineering chemistry research*, *35*(12), pp.4682-4685.

Zhou, X.Y., Cui, Y.F., Jia, D.M. and Xie, D., 2009. Effect of a complex plasticizer on the structure and properties of the thermoplastic PVA/starch blends. *Polymer-Plastics Technology and Engineering*, *48*(5), pp.489-495.

Zou, G.X., Jin, P.Q. and Xin, L.Z., 2008. Extruded starch/PVA composites: Water resistance, thermal properties, and morphology. *Journal of Elastomers & Plastics*, *40*(4), pp.303-316.

Zugenmaier, P., 2008. *Crystalline cellulose and derivatives: characterization and structures*. Springer Science & Business Media.